On the Rate Regions of Single-Channel and Multi-Channel Full-Duplex Links

Jelena Diakonikolas and Gil Zussman

Abstract—**We study the achievable *rate regions of full-duplex links* in the *single- and multi-channel cases* (in the latter case, the channels are assumed to be orthogonal – e.g., OFDM). We present analytical results that characterize the uplink and downlink rate region and efficient algorithms for computing rate pairs at the region's boundary. We also provide near-optimal and heuristic algorithms that "convexify" the rate region when it is not convex. The convexified region corresponds to a combination of a few full-duplex rates (i.e., to time sharing between different operation modes). The algorithms can be used for theoretical characterization of the rate region as well as for resource (time, power, and channel) allocation with the objective of maximizing the sum of the rates when one of them (uplink or downlink) must be guaranteed (e.g., due to QoS considerations). We numerically illustrate the rate regions and the rate gains (compared to time division duplex) for various channel and cancellation scenarios. The analytical results provide insights into the properties of the full-duplex rate region and are essential for future development of scheduling, channel allocation, and power control algorithms.**

Index Terms—**Full-duplex, resource allocation, rate region.**

I. Introduction

Existing wireless systems are Half-Duplex (HD), where separating the transmitted and received signal in either frequency or time causes inefficient utilization of the wireless resources. An emerging technology that can substantially improve spectrum efficiency is Full-Duplex (FD) wireless, namely, simultaneous transmission and reception on the same frequency channel [2]. The main challenge in implementing FD devices is the high Self-Interference (SI) caused by signal leakage from the transmitter into the receiver. The SI signal is usually many orders of magnitude higher than the desired signal at the receiver's input, requiring over 100dB (10^{10} times) of Self-Interference Cancellation (SIC). Recently, several groups demonstrated that combining techniques in the analog and digital domains can provide sufficiently high SIC to support practical applications (e.g., [3]–[9]).

The first implementations of FD receivers optimistically envisioned $2\times$ data rate improvement (e.g., [4], [8]). However, such a rate increase requires perfect SIC, which is extremely challenging to achieve. While a few recent papers considered non-negligible SI and the resulting rate gains [10]–[13], *there is still no explicit characterization of the FD rate region for a given profile of residual SI over frequency*[1] *and parameters of the wireless signal*. Most recent research has focused on maximizing the total throughput without considering Quality of Service (QoS) requirements. Namely, there has been very limited work on asymmetric traffic requirements on the uplink (UL) and downlink (DL) [11], [13]–[15].

A partial and preliminary version of this paper appeared in the Proceedings of ACM MobiHoc'16 [1].

J. Diakonikolas is with the Computer Science dept. at Boston University, Boston, MA, 02215, email: jelenad@bu.edu. The results from this paper were obtained while she was a graduate student at Columbia University.

G. Zussman is with the Electrical Engineering dept., Columbia University, New York, NY, 10027, USA, email: gil@ee.columbia.edu.

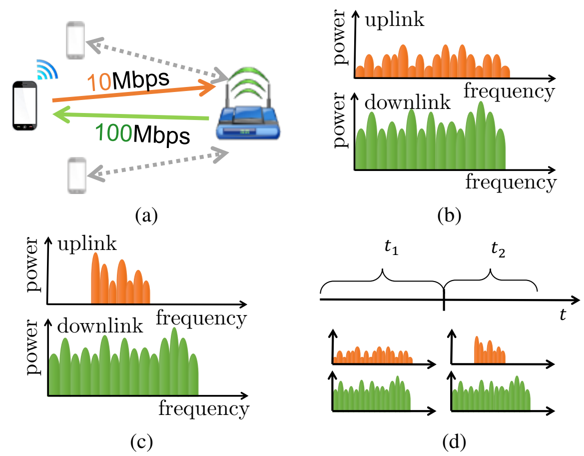

Fig. 1: (a) An example of different rate requirements on a full-duplex link and possible policies to meet the requirements: (b) reduction of the power levels on the UL channels, (c) allocation of a subset of the channels to the UL, and (d) time-sharing between two FD rate pairs (time division full-duplex).

While in Time Division Duplex (TDD) systems asymmetric traffic can be supported via time-sharing between the UL and DL, in FD the dependence of the bi-directional rates on the transmission power levels and Signal-to-Noise Ratio (SNR) levels is much more complex. As shown in Fig. 1, any (combination) of the following policies can be used: (i) FD with reduced transmission power at one of the stations, (ii) FD with fewer channels allocated to one of the stations, and (iii) time sharing between a few types of FD transmissions.

We study asymmetric link traffic and analytically characterize the rate region (i.e., all possible combinations of UL and DL rates) under non-negligible SI. Such a characterization has theoretical importance, since it provides insights into the achievable gains from FD, thereby allowing to quantify the benefits in relation to the costs (in hardware and algorithmic complexity, power consumption, etc.). It also has practical importance, since it supports the development of algorithms for rate allocation under different UL and DL requirements. Such algorithms will determine the required combinations of the policies illustrated in Fig. 1.

[1] In compact FD radio implementations (e.g., [7]), the residual SI can vary wildly with the frequency.

We first consider the case where both stations transmit on a *single channel* and the remaining SI is a constant fraction of the transmitted power [13], [14]. We study the structural properties of the FD rate region and derive necessary and sufficient conditions for its convexity. Based on the properties, we present a simple and fast algorithm to "convexify" the region.[2] The convexified region combines (via time sharing) different FD rate pairs (see Fig. 1(d)) and we refer to it as the Time Division Full-Duplex (TDFD) region. The algorithm finds the points at the region's boundary, given a constraint on one of the (UL or DL) rates.

We then consider the *multi-channel* case in which channels are orthogonal, as in Orthogonal Frequency Division Multiplexing (OFDM). We assume that the *shape of the power allocation is fixed* but the total transmission power can be varied. Namely, the ratios between power levels at different channels are given. For each channel, the residual SI is some fraction of the transmitted power [12], [13], [16]. We characterize the FD rate region and analytically show that any point on the region can be computed with a low-complexity binary search. We also focus on determining the TDFD rate region, which due to the lack of structure cannot in general be obtained via binary search. However, we argue that in practice the TDFD rate region can be determined in real time.

Finally, we consider the TDFD rate region in the *multi-channel* case under a *general power allocation*, (i.e., the power level at each channel is a decision variable). In this case, maximizing one of the rates when the other rate is given is a non-convex problem which is hard to solve in general. However, we develop an algorithm that under certain mild restrictions converges to a stationary point that in practice is a global maximum. Although for most practical cases, the algorithm is near-optimal and runs in polynomial time, its running time is not suitable for a real-time implementation. Hence, we develop a simple heuristic and show numerically that in most cases it has similar performance.

For all the cases mentioned above, we present extensive numerical results that illustrate the rate regions and the rate gains (compared to TDD) as a function of the receivers' SNR levels and SIC levels. We also highlight the intuition behind the performance of the different algorithms.

To summarize, the main contributions of the paper are two-fold: (i) it provides a fundamental characterization and structural understanding of the FD rate regions, and (ii) the rate maximization algorithms, designed for asymmetrical traffic requirements, can serve as resource allocation building blocks for future FD MAC protocols.

The rest of the paper is organized as follows. Sections II and III review related work and outline the model. Section IV studies the single channel case. Sections V and VI study the multi-channel cases with fixed and general power allocations. We conclude in Section VII. Due to space constraints, some of the proofs are omitted and appear in a technical report [17].

[2] A convex region is desirable, since most resource allocation and scheduling algorithms rely on convexity, whereas providing performance guarantees for a non-convex region is generally difficult for the existing techniques.

II. Related Work

Various challenges related to FD wireless recently attracted significant attention. These include FD radio/system design [3]–[8] as well as rate gain evaluation and resource allocation [10]–[14], [16], [18]–[20]. A large body of (analytical) work [18]–[20] focuses on *perfect SIC* while we focus on the more realistic model of imperfect SIC.

Rate gains and power allocation under *imperfect SIC* were studied in [10]–[14], [16]. For the single channel case, [10] derives a sufficient condition for FD to outperform TDD in terms of the sum of UL and DL rates. However, [10] does not quantify the rate gains nor consider the multi-channel case.

Power allocation for maximizing the sum of the UL and DL rates for the single- and multi-channel cases was studied in [12], [13]. The maximization only determines a single point on the rate region and does not imply anything about the rest of the region, which is our focus. While [13] (implicitly) constructs the FD rate region in the single channel case (restated here as Proposition 4.1), it does not derive any structural properties of the region, nor does it consider the multi-channel case or a combination of FD and TDD.

The rate region for an FD MIMO two-way relay channel was studied in [16] as a joint problem of beamforming and power allocation. For a fixed beamforming, the problem reduces to determining a single channel FD rate region. Yet, the joint problem is significantly different from the problems considered here. The multi-channel FD rate region was considered in [11]. While [11] considers both fixed and general power allocations for determining an FD rate region, analytical results are obtained only for the fixed power case while the problem of general power allocation was addressed heuristically.

The TDFD rate region was studied in [15] only via simulation and in [14] analytically but mainly for the single-channel case. The "convexification" of the FD region in [14] is performed over a discrete set of rate pairs, which requires linear computation in the set size, assuming that the points are sorted (e.g., Ch. 33 in [21]). Our results for a single channel rely on the structural properties of the FD rate region and do not require the set of FD rate pairs to be discrete. Moreover, the computation for determining the convexified region is logarithmic (see Section IV-B).

To the best of our knowledge, this is the first thorough study of the rate region and rate gains of FD and TDFD.

III. Model and Notation

We focus on the problem of determining the rate region of an FD bidirectional link between two stations. For brevity, we refer to them as the Mobile Station (MS) and the Base Station (BS) and to the corresponding links as the uplink (UL) and the downlink (DL). While the analytical results apply to an arbitrary pair of FD stations, we choose this terminology to illustrate in numerical evaluations the regions corresponding to a station with more powerful SIC (e.g., an access point or a BS) and a station with less powerful SIC (e.g., a smartphone).

A. Notation

For the number of channels K, we consider: (i) the single-channel case ($K = 1$), and (ii) the multi-channel case ($K > 1$),

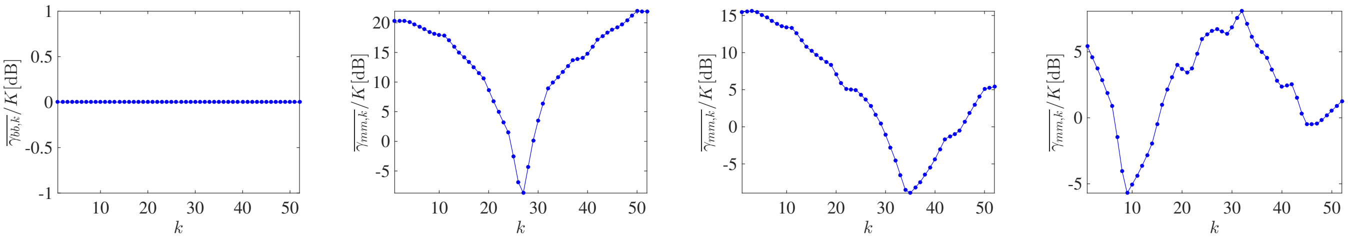

(a) (b) (c) (d)

Fig. 2: Considered cancellation profiles for the FD receiver (a) at the BS [8] and (b), (c), (d) at the MS [7].

TABLE I: Nomenclature.

m	Subscript notation for the MS
b	Subscript notation for the BS
K	Total number of OFDM channels
k	Channel index, $k \in \{1, ..., K\}$
$P_{u,k}$	Transmission power of station u on ch. k, $u \in \{b, m\}$
$\overline{P_u}$	Maximum total power: $\sum_{k=1}^{K} P_{u,k} \leq \overline{P_u}$, $u \in \{b, m\}$
$\alpha_{u,k}$	$= P_{u,k}/\overline{P_u}$, $u \in \{b, m\}$, $\sum_{k=1}^{K} \alpha_{u,k} \leq 1$
$\overline{\gamma_{uv,k}}$	SNR of signal from u to v on channel k, where $u \neq v$, $u, v \in \{m, b\}$, when $\alpha_{u,k} = 1$
$\overline{\gamma_{uu,k}}$	XINR at station u, channel k when $\alpha_{u,k} = 1$, where $u \in \{b, m\}$
r_b	Sum of the rates on the downlink
r_m	Sum of the rates on the uplink
$\overline{r_b}$	Maximum (TDD) rate on the downlink
$\overline{r_m}$	Maximum (TDD) rate on the uplink
(r_b^*, r_m^*)	Target point on the rate region's boundary

where we assume that the channels are orthogonal to each other. In the numerical evaluations, when $K > 1$ we take $K = 52$. We use k to denote the channel index. When $K = 1$, we omit the indices.

$P_{u,k}$ denotes the transmission power level at station $u \in \{m, b\}$ on channel k and $\overline{P_u}$ denotes the maximum sum of transmission power levels at station u: $\sum_{k=1}^{K} P_{u,k} \leq \overline{P_u}$, where $u \in \{m, b\}$. For simplicity, we introduce notation for the normalized transmission power levels: $\alpha_{b,k} = P_{b,k}/\overline{P_b}$, $\alpha_{m,k} = P_{m,k}/\overline{P_m}$. The constraints for the sum of transmission power levels are then: $\sum_k \alpha_{b,k} \leq 1$ and $\sum_k \alpha_{m,k} \leq 1$.

$\overline{\gamma_{bm,k}}$ and $\overline{\gamma_{mb,k}}$ denote the SNR of the signal from the BS to the MS and from the MS to the BS, respectively, on channel k, when the transmission power level on channel k is set to its maximum value ($\overline{P_b}$, $\overline{P_m}$, respectively). Observe that in that case $\alpha_{b,k}$ (respectively, $\alpha_{m,k}$) is equal to 1.

$\overline{\gamma_{bm}} \equiv \frac{1}{K}\sum_k \overline{\gamma_{bm,k}}/K$ and $\overline{\gamma_{mb}} \equiv \frac{1}{K}\sum_k \overline{\gamma_{mb,k}}/K$ denote the average SNR when the power levels are equally allocated over channels (i.e., when $\alpha_{b,1} = ... = \alpha_{b,K} = 1/K$ and $\alpha_{m,1} = ... = \alpha_{m,K} = 1/K$). In the numerical evaluations, we take $\overline{\gamma_{bm,k}} = K\overline{\gamma_{bm}}$ and $\overline{\gamma_{mb,k}} = K\overline{\gamma_{mb}}$, $\forall k$, to focus on the effects caused by FD operation. Our results, however, hold for general values of $\overline{\gamma_{bm,k}}$ and $\overline{\gamma_{mb,k}}$ over channels k.

Similarly to [11]–[13], we model the remaining SI on channel k as a constant fraction of the transmission power level on channel k. The Self-Interference-to-Noise-Ratio (XINR) at the BS on channel k when $\alpha_{b,k} = 1$ is denoted by $\overline{\gamma_{bb,k}}$. The XINR at the MS on channel k when $\alpha_{m,k} = 1$ is denoted by $\overline{\gamma_{mm,k}}$. In the numerical evaluations of the multi-channel case, we use $\overline{\gamma_{bb,k}}/K = 1 = 0$dB, as shown in Fig. 2(a), which

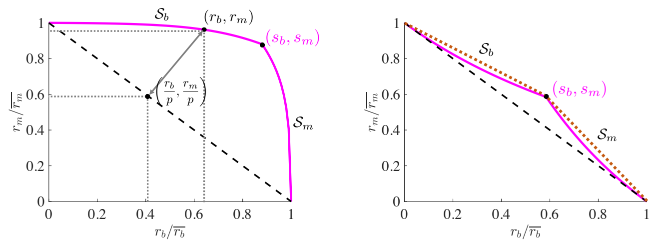

(a) (b)

Fig. 3: (a) Convex and (b) non-convex FD rate regions. A dashed line delimits the corresponding TDD region. An FD region is convex, if and only if segments $\mathcal{S}_b$ (connecting $(0, \overline{r_m})$ and (s_b, s_m)) and $\mathcal{S}_m$ (connecting (s_b, s_m) and $(\overline{r_b}, 0)$) can be represented by a concave function $r_m(r_b)$.

is motivated by [8]. For $\overline{\gamma_{mm,k}}$, we consider three FD RFIC designs from [7], shown in Fig. 2(b)–(d). For the FD RFICs from [7], we assume additional 50dB of cancellation in the digital domain and 110dB difference between the maximum transmission signal and the noise.

We denote the DL rate on channel k by $r_{b,k}$ and the UL rate on channel k by $r_{m,k}$. The sum of the rates over channels on the DL (resp. UL) is denoted by $r_b = \sum_k r_{b,k}$ (resp. $r_m = \sum_k r_{m,k}$), and we let $r = r_m + r_b$ denote the sum of all UL and DL rates over channels k (in the following, we refer to r as the sum rate). We denote by $\overline{r_b} = \max\{r_b(\{\alpha_{b,k}\}, \{\alpha_{m,k}\}) : \sum_k \alpha_{b,k} \leq 1, \sum_k \alpha_{m,k} \leq 1\}$ the maximum DL rate. Observe that when r_b is maximized, we have $\sum_k \alpha_{b,k} = 1, \alpha_{m,k} = 0, \forall k$, i.e., $\overline{r_b}$ is equal to the maximum HD rate on the DL. Similarly, $\overline{r_m}$ denotes the maximum UL rate.

Summary of the main notation is provided in Table I.

B. Main Definitions

To determine $r_{b,k}$ and $r_{m,k}$, we use the Shannon's capacity formula: $r_{b,k} = \log\left(1 + \frac{\alpha_{b,k}\overline{\gamma_{bm,k}}}{1+\alpha_{m,k}\overline{\gamma_{mm,k}}}\right)$, $r_{m,k} = \log\left(1 + \frac{\alpha_{m,k}\overline{\gamma_{mb,k}}}{1+\alpha_{b,k}\overline{\gamma_{bb,k}}}\right)$, where log denotes the base-2 logarithm. Thus, the UL and DL rates are always functions of the power allocation $\{\alpha_{b,k}\}, \{\alpha_{m,k}\}$. Whenever the power allocation is clear from the context, we will omit explicitly denoting the rates as functions of the power allocation.

A rate region of an FD link is the set of all achievable UL-DL FD rate pairs. Examples of FD regions appear in Fig. 3, where a full line represents the FD region boundary, and a dashed line represents the TDD region boundary. *The problem of determining the FD rate region is the problem of*

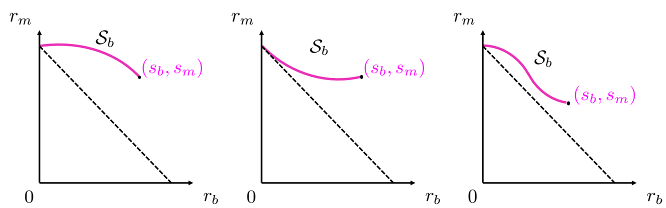

Fig. 4: Possible shapes of segments $\mathcal{S}_b$ and $\mathcal{S}_m$: (a) concave, (b) convex, (c) concave and then convex.

maximizing one of the rates (e.g., r_m) when the other rate (r_b) is fixed, subject to the sum power constraints.

An FD rate region is not necessarily convex. In such cases, we also consider a *convexified* or *TDFD* rate region, namely, the convex hull of the FD rate region. In practice, the TDFD region would correspond to time sharing between different FD rate pairs. Fig. 3(b) illustrates a non-convex FD rate region, with the dotted line representing the boundary of the TDFD rate region. To compare an FD or a TDFD rate region to its corresponding TDD region, we use the following definition (a similar definition appears in [13], see Fig. 3(a) for intuition):

Definition 3.1: For a given rate pair (r_b, r_m) from an FD or TDFD rate region, the rate improvement p is defined as the (positive) number for which $\left(\frac{r_b}{p}, \frac{r_m}{p}\right)$ is at the boundary of the corresponding TDD rate region.

Using simple geometry, p can be computed as follows [13]:

Proposition 3.2: $p(r_b, r_m) = r_b/\overline{r_b} + r_m/\overline{r_m}$.

IV. Single Channel

We now study the structural properties of the FD and TDFD rate regions for a single FD channel and devise an algorithm that determines the points at the boundary of the TDFD rate region. First, we provide structural results that characterize FD rate regions. We prove that the FD region boundary, which can be described by an implicit function $r_m(r_b)$[3], can only have up to four either convex or concave pieces that can only appear in certain specific arrangements. We also provide necessary and sufficient conditions for the region's boundary to take one of the possible shapes. As a corollary, we derive necessary and sufficient conditions for the FD region to be convex as a function of $\overline{\gamma_{bm}}, \overline{\gamma_{mb}}, \overline{\gamma_{mm}}$, and $\overline{\gamma_{bb}}$.

Based on the structural results, we present a simple and fast algorithm that can determine any point at the boundary of the TDFD rate region. For a given rate r_b^*, to find the maximum rate r_m subject to $r_b = r_b^*$, the algorithm determines the shape of the rate region as a function of $\overline{\gamma_{bm}}, \overline{\gamma_{mb}}, \overline{\gamma_{mm}}$, and $\overline{\gamma_{bb}}$, and either directly computes r_m or finds it via a binary search.

A. Rate Region Structural Results

We start by characterizing the power allocation at the boundary of an FD rate region, given by the following simple proposition (used implicitly in [13]). The proof appears in [17]. In the rest of the section, $s_b = r_b(1,1)$, $s_m = r_m(1,1)$.

[3]Note that r_b and r_m are both functions of the power allocation. Here, $r_m(r_b)$ refers to the values of r_m when r_b is fixed and r_m is maximized.

Proposition 4.1: If $r_b = r_b^* \leq s_b$, then r_m is maximized for $\alpha_m = 1$ and α_b that solves $r_b(\alpha_b, 1) = r_b^*$. Similarly, if $r_m = r_m^* \leq s_m$, then r_b is maximized for $\alpha_b = 1$ and α_m that solves $r_m(1, \alpha_m) = r_m^*$.

Using Proposition 4.1, the FD rate region can be determined as in Algorithm 1 (SC-FD-Region).

Algorithm 1 SC-FD-Region(r_b^*)

Input: $\overline{\gamma_{mm}}, \overline{\gamma_{bb}}, \overline{\gamma_{mb}}, \overline{\gamma_{bm}}$
if $r_b \leq r_b^*$ **then**
  $\alpha_b = (2^{r_b^*} - 1)(1 + \overline{\gamma_{mm}})/\overline{\gamma_{bm}}$
  $r_m^* = \log(1 + \frac{\overline{\gamma_{mb}}}{1+\alpha_b\overline{\gamma_{bb}}})$
else
  $\alpha_m = (\overline{\gamma_{bm}}/(2^{r_b^*} - 1) - 1)/\overline{\gamma_{mm}}$
  $r_m^* = \log(1 + \frac{\alpha_m\overline{\gamma_{mb}}}{1+\overline{\gamma_{bb}}})$
return r_m^*

The rate region is convex, if and only if (i) $r_b(r_m)$ is concave for $r_m \in (0, s_m]$ and r_b at the boundary of the rate region, (ii) $r_m(r_b)$ is concave for $r_b \in (0, s_b]$ and r_m at the boundary of the rate region, and (iii) the functions $r_m(r_b)$ and $r_b(r_m)$ intersect at (s_b, s_m) under an angle smaller than π (see Fig. 5 for an illustration of why (iii) is important).

If the FD rate region is convex (Fig. 3(a)), then to maximize r_m subject to $r_b = r_b^*$, it is always optimal to use FD and allocate the power levels according to Proposition 4.1. This is not necessarily true, if the rate region is not convex; in that case, it may be optimal to use a time-sharing scheme between two FD rate pairs (TDFD), since a convex combination of e.g., (s_b, s_m) and $(\overline{r_b}, 0)$ may lie above the FD rate region boundary (e.g., Fig. 3(b)).

The following lemma characterizes the FD rate region boundary. The lemma states that each of the segments $\mathcal{S}_b$ (corresponding to $r_m(r_b)$ at the boundary of the FD rate region for $r_b \in [0, s_b]$) and $\mathcal{S}_m$ (corresponding to $r_b(r_m)$ at the boundary of the FD rate region for $r_m \in [0, s_m]$) can only take one of the three possible shapes illustrated in Fig. 4.

Lemma 4.2: Given positive $\overline{\gamma_{mb}}, \overline{\gamma_{bm}}, \overline{\gamma_{bb}}, \overline{\gamma_{mm}}$, let $\mathcal{S}_b$ describe the boundary of the FD rate region for $r_b \in [0, s_b]$, and $\mathcal{S}_m$ describe the boundary of the FD rate region for $r_m \in [0, s_m]$. Then $\mathcal{S}_b$ and $\mathcal{S}_m$ can only be described by one of the following three function types: (i) concave, (ii) convex, and (iii) concave for $r_b \in [0, r_b^+]$ for some $r_b^+ < s_b$ in the case of $\mathcal{S}_b$, concave for $r_m \in [0, r_m^+]$ for some $r_m^+ < s_m$ in the case of $\mathcal{S}_m$, and convex on the rest of the domain.

Proof: From Prop. 4.1, segment $\mathcal{S}_b$ is described by $r_m(r_b)$, where $r_b \leq s_b$, $\alpha_b \in [0, 1]$, and:

$$r_b = \log\left(1 + \frac{\alpha_b\overline{\gamma_{bm}}}{1 + \overline{\gamma_{mm}}}\right), \; r_m = \log\left(1 + \frac{\overline{\gamma_{mb}}}{1 + \alpha_b\overline{\gamma_{bb}}}\right). \quad (1)$$

Similarly, segment $\mathcal{S}_m$ is described by $r_b(r_m)$, where $r_m \leq s_m$, $\alpha_m \in [0, 1]$, and:

$$r_b = \log\left(1 + \frac{\overline{\gamma_{bm}}}{1 + \alpha_m\overline{\gamma_{mm}}}\right), \; r_m = \log\left(1 + \frac{\alpha_m\overline{\gamma_{mb}}}{1 + \overline{\gamma_{bb}}}\right). \quad (2)$$

We prove the lemma only for segment $\mathcal{S}_b$, while the proof for segment $\mathcal{S}_m$ follows by symmetry.

Since, from (1), $r_m(r_b)$ is a continuous and twice differentiable function for $r_b \in [0, s_b]$ (equivalently, $\alpha_b \in [0,1]$), $r_m(r_b)$ is concave for $r_b \in [0, s_b]$ if and only if $\frac{d^2 r_m}{d{r_b}^2} \leq 0$. Observe that we can write:

$$\frac{dr_m}{dr_b} = \frac{dr_m}{d\alpha_b} \cdot \frac{d\alpha_b}{dr_b} \tag{3}$$

and

$$\frac{d^2 r_m}{d{r_b}^2} = \frac{d^2 r_m}{d{\alpha_b}^2} \cdot \left(\frac{d\alpha_b}{dr_b}\right)^2 + \frac{dr_m}{d\alpha_b} \cdot \frac{d^2\alpha_b}{d{r_b}^2}. \tag{4}$$

From the left equality in (1):

$$\alpha_b = (2^{r_b} - 1) \cdot \frac{1 + \overline{\gamma_{mm}}}{\overline{\gamma_{bm}}},$$

$$\frac{d\alpha_b}{dr_b} = \ln(2) \cdot 2^{r_b} \cdot \frac{1 + \overline{\gamma_{mm}}}{\overline{\gamma_{bm}}}, \text{ and} \tag{5}$$

$$\frac{d^2\alpha_b}{d{r_b}^2} = \ln^2(2) \cdot 2^{r_b} \cdot \frac{1 + \overline{\gamma_{mm}}}{\overline{\gamma_{bm}}}. \tag{6}$$

From the right equality in (1):

$$\frac{dr_m}{d\alpha_b} = -\frac{\overline{\gamma_{bb}}}{\ln(2)} \cdot \Big(\frac{1}{1 + \alpha_b\overline{\gamma_{bb}}} - \frac{1}{1 + \alpha_b\overline{\gamma_{bb}} + \overline{\gamma_{mb}}}\Big), \tag{7}$$

$$\frac{d^2 r_m}{d{\alpha_b}^2} = \frac{(\overline{\gamma_{bb}})^2}{\ln(2)} \cdot \Big(\frac{1}{1 + \alpha_b\overline{\gamma_{bb}}} - \frac{1}{1 + \alpha_b\overline{\gamma_{bb}} + \overline{\gamma_{mb}}}\Big) \cdot \Big(\frac{1}{1 + \alpha_b\overline{\gamma_{bb}}} + \frac{1}{1 + \alpha_b\overline{\gamma_{bb}} + \overline{\gamma_{mb}}}\Big). \tag{8}$$

Plugging (5)–(8) back into (4), we have that the sign of $\frac{d^2 r_m}{d{r_b}^2}$ is equivalent to the sign of:

$$\overline{\gamma_{bb}}\Big(\frac{1}{1 + \alpha_b\overline{\gamma_{bb}}} + \frac{1}{1 + \alpha_b\overline{\gamma_{bb}} + \overline{\gamma_{mb}}}\Big)\frac{2^{r_b}(1 + \overline{\gamma_{mm}})}{\overline{\gamma_{bm}}} - 1. \tag{9}$$

Recalling (from (1)) that $2^{r_b} = 1 + \frac{\alpha_b\overline{\gamma_{bm}}}{1+\overline{\gamma_{mm}}}$ and using simple algebraic transformations, (9) is equivalent to:

$${\alpha_b}^2 + \alpha_b\frac{2(1 + \overline{\gamma_{mm}})}{\overline{\gamma_{bm}}} + \frac{(2 + \overline{\gamma_{mb}})(1 + \overline{\gamma_{mm}})}{\overline{\gamma_{bb}}\,\overline{\gamma_{bm}}} - \frac{1 + \overline{\gamma_{mb}}}{(\overline{\gamma_{bb}})^2}. \tag{10}$$

(10) is a quadratic function whose smaller root is negative. If the discriminant of (10) is negative or the larger root is at most 0, (10) is non-negative for all $\alpha_b \in [0,1]$, and therefore $r_m(r_b)$ is convex for all $r_b \in [0, s_b]$. If the discriminant of (10) is positive and the larger root is at least 1, (10) is non-positive for all $\alpha_b \in [0,1]$, and therefore $r_m(r_b)$ is concave for all $r_b \in [0, s_b]$. Finally, if the discriminant of (10) is positive and the larger root takes value $\alpha_b^+ < 1$, $r_m(r_b)$ is concave for $r_b \in [0, r_b^+]$ and convex for $r_b \in [r_b^+, s_b]$, where $r_b^+ = r_b(\alpha_b^+, 1)$. ■

The following corollary of the proof of Lemma 4.2 gives necessary and sufficient conditions for $\mathcal{S}_b$ to be concave, and, similarly, for $\mathcal{S}_m$ to be concave. The proof is provided in Appendix A.

Corollary 4.3: For given positive $\overline{\gamma_{mb}}, \overline{\gamma_{bm}}, \overline{\gamma_{bb}}$, and $\overline{\gamma_{mm}}$, $\mathcal{S}_b$ is concave if and only if:

$$\overline{\gamma_{bm}} > \max\Big\{(\overline{\gamma_{mm}})^2 - 1,\ \overline{\gamma_{bb}}(1 + \overline{\gamma_{mm}})\frac{2 + \overline{\gamma_{mb}}}{1 + \overline{\gamma_{mb}}}, (1 + \overline{\gamma_{mm}})\frac{2 + (2 + \overline{\gamma_{mb}})/\overline{\gamma_{bb}}}{(1 + \overline{\gamma_{mb}})/(\overline{\gamma_{bb}})^2 - 1}\Big\}. \tag{11}$$

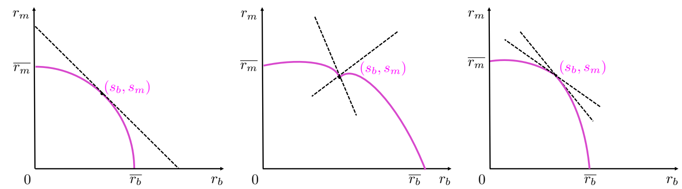

(a) (b) (c)

Fig. 5: Possible intersections of $r_m(r_b)$ and $r_b(r_m)$ at (s_b, s_m): (a) $-\Big(\frac{dr_b}{dr_m}\Big|_{r_m=s_m}\Big)^{-1} = -\frac{dr_m}{dr_b}\Big|_{r_b=s_b}$, (b) $-\Big(.\frac{dr_b}{dr_m}\Big|_{r_m=s_m}\Big)^{-1} < -\frac{dr_m}{dr_b}\Big|_{r_b=s_b}$, and (c) $-\Big(\frac{dr_b}{dr_m}\Big|_{r_m=s_m}\Big)^{-1} > -\frac{dr_m}{dr_b}\Big|_{r_b=s_b}$.

Similarly, $\mathcal{S}_m$ is concave if and only if:

$$\overline{\gamma_{mb}} > \max\Big\{(\overline{\gamma_{bb}})^2 - 1,\ \overline{\gamma_{mm}}(1 + \overline{\gamma_{bb}})\frac{2 + \overline{\gamma_{bm}}}{1 + \overline{\gamma_{bm}}}, (1 + \overline{\gamma_{bb}})\frac{2 + (2 + \overline{\gamma_{bm}})/\overline{\gamma_{mm}}}{(1 + \overline{\gamma_{bm}})/(\overline{\gamma_{mm}})^2 - 1}\Big\}. \tag{12}$$

Finally, we show that whenever both $\mathcal{S}_b$ and $\mathcal{S}_m$ are concave, the FD region is convex.

Lemma 4.4: If both $\mathcal{S}_b$ and $\mathcal{S}_m$ are concave, then the FD rate region is convex.

Proof: Showing that the FD rate region is convex is equivalent to showing that whenever (11)–(12) hold, $r_m(r_b)$ and $r_b(r_m)$ intersect over an angle that is at most π at the point (s_b, s_m). (That is to say, the tangents of $r_m(r_b)$ and $r_b(r_m)$ at (s_b, s_m) form an angle that is at most π.)

Observe the derivative of $r_m(r_b)$ with respect to r_b at $r_b = s_b$ (equivalently $\alpha_b = 1$). From (3), (5), and (7):

$$\frac{dr_m}{dr_b}\Big|_{r_b=s_b} = \Big(\frac{dr_m}{d\alpha_b} \cdot \frac{d\alpha_b}{dr_b}\Big)\Big|_{\alpha_b=1} = -\frac{1 + \overline{\gamma_{mm}} + \overline{\gamma_{bm}}}{1 + \overline{\gamma_{bb}} + \overline{\gamma_{mb}}} \cdot \frac{\overline{\gamma_{bb}}}{1 + \overline{\gamma_{bb}}} \cdot \frac{1}{\overline{\gamma_{bm}}}.$$

Symmetrically:

$$\frac{dr_b}{dr_m}\Big|_{r_m=s_m} = -\frac{1 + \overline{\gamma_{bb}} + \overline{\gamma_{mb}}}{1 + \overline{\gamma_{mm}} + \overline{\gamma_{mb}}} \cdot \frac{\overline{\gamma_{mm}}}{1 + \overline{\gamma_{mm}}} \cdot \frac{1}{\overline{\gamma_{mb}}}.$$

Observe that both $\frac{dr_m}{dr_b}\Big|_{r_b=s_b} < 0$ and $\frac{dr_b}{dr_m}\Big|_{r_m=s_m} < 0$. Whenever $r_m(r_b)$ is concave and $r_b(r_m)$ is concave, for the rate region to be convex it is necessary and sufficient that (see Fig. 5):

$$\Big(-\frac{dr_b}{dr_m}\Big|_{r_m=s_m}\Big)^{-1} \geq -\frac{dr_m}{dr_b}\Big|_{r_b=s_b}$$
$$\Leftrightarrow\ \overline{\gamma_{mb}} \cdot \frac{1 + \overline{\gamma_{mm}}}{\overline{\gamma_{mm}}} \geq \frac{\overline{\gamma_{bb}}}{1 + \overline{\gamma_{bb}}} \cdot \frac{1}{\overline{\gamma_{bm}}}$$
$$\Leftrightarrow\ \overline{\gamma_{bm}}\,\overline{\gamma_{mb}} \geq \frac{\overline{\gamma_{mm}}\,\overline{\gamma_{bb}}}{(1 + \overline{\gamma_{mm}})(1 + \overline{\gamma_{bb}})}. \tag{13}$$

Recall (from (27)) that for $r_m(r_b)$ to be concave, it must be:

$$\overline{\gamma_{bm}} > \overline{\gamma_{bb}}(1 + \overline{\gamma_{mm}})\frac{2 + \overline{\gamma_{mb}}}{1 + \overline{\gamma_{mb}}} > \overline{\gamma_{bb}}(1 + \overline{\gamma_{mm}}) \geq \frac{\overline{\gamma_{bb}}}{1 + \overline{\gamma_{mm}}}. \tag{14}$$

Symmetrically:

$$\overline{\gamma_{bm}} > \frac{\overline{\gamma_{mm}}}{1 + \overline{\gamma_{bb}}}. \tag{15}$$

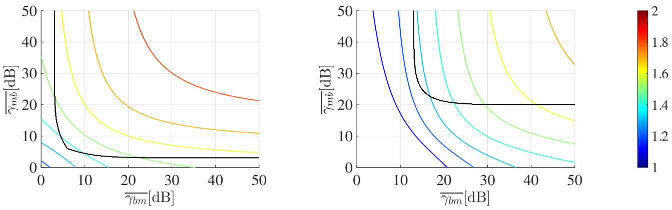

(a) $\overline{\gamma_{mm}} = 0$dB (b) $\overline{\gamma_{mm}} = 10$dB

Fig. 6: Convexity of the rate region vs. rate improvement for $\overline{\gamma_{bb}} = 0$dB and: (a) $\overline{\gamma_{mm}} = 0$dB and (b) $\overline{\gamma_{mm}} = 10$dB. The rate region is convex for UL and DL SNRs north and east from the black curve.

Combining (14) and (15) gives (13), and therefore, the rate region is convex whenever $r_m(r_b)$ and $r_b(r_m)$ are both concave (which is equivalent to (11), (12) both being true). ■

To summarize the results from this section, in Algorithm 2 we provide a procedure for determining the shape of the FD rate region. To encode the shape of $\mathcal{S}_b$ and $\mathcal{S}_m$ we assign them each a two-bit number, where $[1, 1]$ means that $\mathcal{S}_b$ (resp. $\mathcal{S}_m$) is concave, $[1, 0]$ means it is concave then convex, and $[0, 0]$ means that it is convex. We have already proved in Lemma 4.2 that these are the only possible cases. We also return two additional values r_b^+ and r_m^+. If $\mathcal{S}_b = [1, 0]$, r_b^+ is the value of r_b at which $\mathcal{S}_b$ changes the shape from concave to convex. If $\mathcal{S}_b = [1, 1]$, $r_b^+ = s_b$, and otherwise $r_b^+ = 0$. The value r_m^+ is determined similarly, by considering $\mathcal{S}_m$ instead of $\mathcal{S}_b$.

Algorithm 2 SC-RR-SHAPE

```
Input: γmm, γbb, γmb, γbm
if (10) does not have real roots or the larger root is negative then
    S_b = [0,0], r_b^+ = 0
else
    Let α_b^+ be the larger root of (10)
    if α_b^+ ≥ 1 then
        S_b = [1,1], r_b^+ = s_b
    else
        S_b = [1,0], r_b^+ = log(1 + α_b^+ γbb / (1+γmm))
Perform symmetrical procedure for S_m, r_m^+
return S_b, r_b^+, S_m, r_m^+
```

Fig. 6 illustrates the regions of (maximum) SNR values $\overline{\gamma_{bm}}$ and $\overline{\gamma_{mb}}$ for which the FD rate region is convex, for different values of $\overline{\gamma_{mm}}$ and $\overline{\gamma_{bb}}$, compared to the maximum achievable rate improvements. The black line delimits the region of $\overline{\gamma_{bm}}$ and $\overline{\gamma_{mb}}$ for which the FD region is convex: north and east from it, the region is convex, while south and west from it, the region is not convex. As Fig. 6 suggests, *high (over* $1.6\times$*) rate improvements are mainly achievable in the area where the FD region is convex, unless one of the SNR values* $\overline{\gamma_{bm}}$ *and* $\overline{\gamma_{mb}}$ *is much higher than the other one.*

B. Determining TDFD rate Region

We now turn to the problem of allocating UL and DL rates, possibly through a combination of FD and TDD, which is equivalent to determining the TDFD rate region. As before, the problem is to maximize r_m subject to $r_b = r_b^*$ and the power constraints. Denote the maximum r_m such that $r_b = r_b^*$ as r_m^*. We start by providing two technical propositions that will determine "allowed" arrangements in which the three possible shapes of $\mathcal{S}_b$ and $\mathcal{S}_m$ can appear.

Proposition 4.5: If (s_b, s_m) maximizes the sum of UL and DL rates, then $(s_b, s_m) \geq \lambda(r_b', r_m') + (1-\lambda)(r_b'', r_m'')$ element-wise for any $\lambda \in [0, 1]$, and any two feasible rate pairs (r_b', r_m') and (r_b'', r_m'').

Proof: Suppose that for some $\lambda \in [0, 1]$ and some pairs of feasible rates (r_b', r_m') and (r_b'', r_m''): $(s_b, s_m) < \lambda(r_b', r_m') + (1-\lambda)(r_b'', r_m'')$. Then either $(r_b', r_m') > (s_b, s_m)$ or $(r_b'', r_m'') > (s_b, s_m)$, and therefore $r_b' + r_m' > s_b + s_m$ or $r_b'' + r_m'' > s_b + s_m$, which is a contradiction, as $s_b + s_m$ maximizes the sum of the (UL and DL) rates. ■

Proposition 4.5 implies that if (s_b, s_m) maximizes the sum of uplink and downlink rates, it must dominate any convex combination of other points from the rate region.

Proposition 4.6: If $s_b + s_m < \overline{r_m}$, then $r_m(r_b)$ is convex on the entire segment from $(0, \overline{r_m})$ to (s_b, s_m). Similarly, if $s_b + s_m < \overline{r_b}$, then $r_b(r_m)$ is convex on the entire segment from (s_b, s_m) to $(\overline{r_b}, 0)$.

The proof can be found in [17].

From Lemma 4.2 and Propositions 4.5 and 4.6, only the following cases can happen:

Case 1: (s_b, s_m) maximizes the sum of the (UL and DL) rates. Then, using Proposition 4.5: (i) if $\mathcal{S}_b$ is convex, then (r_b^*, r_m^*) is on the boundary of TDFD (but not FD) rate region and can be found as a convex combination of $(0, \overline{r_m})$ and (s_b, s_m), (ii) if $\mathcal{S}_b$ is concave, (r_b^*, r_m^*) is on the boundary of FD rate region and can be found using Proposition 4.1, and (iii) if $\mathcal{S}_b$ is part-concave-part-convex, then (r_b^*, r_m^*) may be either on the boundary of FD region or TDFD region.

Case 2: (s_b, s_m) does not maximize the sum of the (UL and DL) rates. Suppose w.l.o.g. that $(\overline{r_b}, 0)$ maximizes the sum rate.[4] Then, from Proposition 4.6, $\mathcal{S}_m$ is convex and we have the following cases: (i) if $\mathcal{S}_b$ is convex, then (r_b^*, r_m^*) is either on the boundary of TDD region or on the line connecting $(0, \overline{r_m})$ and (s_b, s_m), (ii) if $\mathcal{S}_b$ is concave, then (r_b^*, r_m^*) is either on the boundary of FD rate region or on the line that contains $(\overline{r_b}, 0)$ and is tangent to $\mathcal{S}_b$, and (iii) if $\mathcal{S}_b$ is part-concave-part-convex, then (r_b^*, r_m^*) may lie either on the boundary of FD or TDFD rate region.

As illustrated in Cases 1 and 2, we can often determine (r_b^*, r_m^*) in constant time, if this point is guaranteed to be either on the boundary of FD rate region, or if we know exactly which two points produce (r_b^*, r_m^*) on the boundary of TDFD rate region as their convex combination. However, there are also cases (Cases 1(iii), 2(ii), and 2(iii)) when it is not immediately clear how to determine (r_b^*, r_m^*). In the following lemma, we show that in such cases we can "convexify" the FD rate region (i.e., determine TDFD rate region) efficiently. Note that the convexification needs to be performed only once; after that, $\mathcal{S}_b$ (and $\mathcal{S}_m$) can be represented in a black-box manner, requiring constant computation to determine any rate pair (r_b^*, r_m^*), given either r_b^* or r_m^*.

[4]The assumption is w.l.o.g. because [13] proved that one of the following three rate pairs maximizes the sum rate $(\overline{r_b}, 0)$, $(0, \overline{r_m})$ or (s_b, s_m).

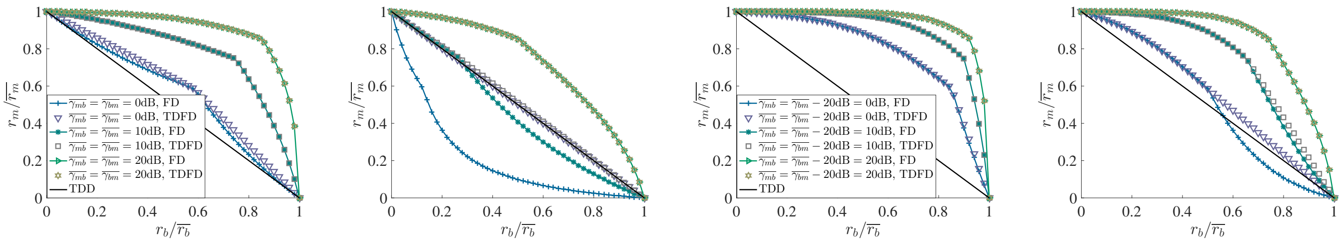

(a) $\overline{\gamma_{bb}} = 0$dB, $\overline{\gamma_{mm}} = 0$dB (b) $\overline{\gamma_{bb}} = 0$dB, $\overline{\gamma_{mm}} = 10$dB (c) $\overline{\gamma_{bb}} = 0$dB, $\overline{\gamma_{mm}} = 0$dB (d) $\overline{\gamma_{bb}} = 0$dB, $\overline{\gamma_{mm}} = 10$dB

Fig. 7: Rate regions for (a), (b) $\overline{\gamma_{bm}} = \overline{\gamma_{mb}}$ and (c), (d) $\overline{\gamma_{bm}} > \overline{\gamma_{mb}}$.

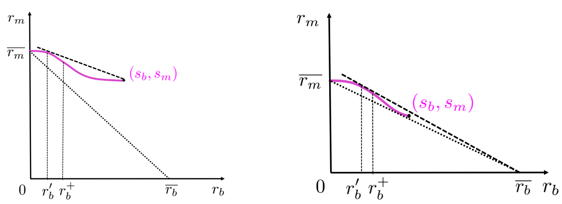

(a) (b)

Fig. 8: Two possible scenarios for Case 2(iii).

Theorem 4.7: The boundary of the TDFD rate region can be determined in time $O(\log(\varepsilon^{-1}\overline{r_b}))$, where ε is the additive error of $r_m^* = \max\{r_m : r_b = r_b^*\}$, and the binary search, if employed, takes at most $\lceil \log(\varepsilon^{-1} \cdot 1.4\overline{r_b}) \rceil$ steps.

Proof: Note that the time to determine r_m^* on the boundary of TDFD rate region may not be constant only in Cases 1(iii), 2(ii), and 2(iii). We start with the Case 1(iii).

Let r_b^+ denote the value of r_b at which $\mathcal{S}_b$ changes the shape from concave to convex, as in Lemma 4.2. Using Proposition 4.5 and simple geometric arguments, it follows that in the "convexified" rate region there exists $r_b' \le r_b^+$ such that the boundary of the region is equal to $r_m(r_b)$ for $r_b \in [0, r_b']$ joined with a line segment from a point $(r_b', r_m(r_b'))$ to (s_b, s_m), where the line through points $(r_b', r_m(r_b'))$ and (s_b, s_m) is tangent to $r_m(r_b)$ at point $(r_b', r_m(r_b'))$ (see Fig. 8(a)). Since the tangent from (s_b, s_m) onto $r_m(r_b)$ must touch $r_m(r_b)$ at a point $(r_b', r_m(r_b'))$ where $r_m(r_b)$ is concave, it follows that we can find r_b' by performing a binary search over $r_b \in [0, r_b^+]$, since every concave function has a monotonically decreasing derivative. It follows that $r_m^* = r_m(r_b^*)$ if $r_b^* \le r_b'$, and $r_m^* = r_m(r_b') + \frac{dr_m}{dr_b}\big|_{r_b = r_b'}(r_b^* - r_b')$ otherwise.

Consider now Case 2(iii), and recall that in this case $s_b + s_m < \overline{r_b}$. Using the same approach as described above, we can determine a point $r_b' \le r_b^+$ such that the line through $(r_b', r_m(r_b'))$ and (s_b, s_m) is tangent to $r_m(r_b)$. However, this approach may not always lead to the convexified region.

Consider the scenario illustrated in Fig. 8(b). From Proposition 4.6, $r_b(r_m)$ for $r_m \in [0, s_m]$ must be convex, and therefore there exists an $r_b'' \le r_b^+$ such that the boundary of the convexified rate region is determined by $r_m(r_b)$ for $r_b \in [0, r_b'']$ and by a line through $(r_b'', r_m(r_b''))$ and (s_b, s_m) for $r_b \in [r_b'', s_b]$, where the line through $(r_b'', r_m(r_b''))$ and (s_b, s_m) is tangent onto $r_m(r_b)$ at point $r_b = r_b''$. Since r_b'' must belong to the segment where $r_m(r_b)$ is concave, it follows that r_b'' can be found through a binary search over $r_b \in [0, r_b^+]$. To determine which one of the two tangents delimits the convexified rate region, it is sufficient to compare $r_m(r_b') + \frac{dr_m}{dr_b}\big|_{r_b = r_b'}(s_b - r_b')$ and $r_m(r_b'') + \frac{dr_m}{dr_b}\big|_{r_b = r_b''}(s_b - r_b'')$ and choose the one with the maximum value.

The proofs for Case 2(ii) and scenarios when $(0, \overline{r_m})$ maximizes the sum rate are similar and are omitted for brevity.

Finally, we show that the binary search can be implemented with low running time. To do so, we first bound the change in the derivative $\frac{dr_m}{dr_b}$ on the segment where $r_m(r_b)$ is concave.

Proposition 4.8: For all $r_b \in [0, s_b]$ such that $r_m(r_b)$ is concave: $\left|\frac{d^2 r_m}{dr_b^2}\right| < 1.4$.

Proof: Fix any r_b such that $r_m(r_b)$ is concave, and let α_b be such that $r_b = r_b(\alpha_b, 1)$. The proof of Lemma 4.2 implies that (using Eq.'s (4)–(9)):

$$\begin{aligned}
\left|\frac{d^2 r_m}{dr_b^2}\right| \le & \frac{\overline{\gamma_{bb}}}{\ln(2)}\left(\frac{1}{1+\alpha_b\overline{\gamma_{bb}}} - \frac{1}{1+\alpha_b\overline{\gamma_{bb}}+\overline{\gamma_{mb}}}\right) \\
& \cdot \ln^2(2) \cdot 2^{r_b}\frac{1+\overline{\gamma_{mm}}}{\overline{\gamma_{bm}}} \\
= & \ln(2)\overline{\gamma_{bb}} \cdot \frac{\overline{\gamma_{mb}}}{(1+\alpha_b\overline{\gamma_{bb}})(1+\alpha_b\overline{\gamma_{bb}}+\overline{\gamma_{mb}})} \\
& \cdot \left(\alpha_b + \frac{1+\overline{\gamma_{mm}}}{\overline{\gamma_{bm}}}\right) \\
< & \ln(2)\frac{\overline{\gamma_{bb}}}{1+\alpha_b\overline{\gamma_{bb}}}\left(\alpha_b + \frac{1+\overline{\gamma_{mm}}}{\overline{\gamma_{bm}}}\right) \\
= & \ln(2)\left(\frac{\alpha_b\overline{\gamma_{bb}}}{1+\alpha_b\overline{\gamma_{bb}}} + \frac{\overline{\gamma_{bb}}(1+\overline{\gamma_{mm}})}{\overline{\gamma_{bm}}} \cdot \frac{1}{1+\alpha_b\overline{\gamma_{bb}}}\right) \\
\le & 2\ln(2) < 1.4,
\end{aligned}$$

where we have used: $\frac{\overline{\gamma_{mb}}}{1+\alpha_b\overline{\gamma_{bb}}+\overline{\gamma_{mb}}} \le \frac{\overline{\gamma_{mb}}}{1+\overline{\gamma_{mb}}} < 1$, $\frac{\alpha_b\overline{\gamma_{bb}}}{1+\alpha_b\overline{\gamma_{bb}}} < 1$, $\frac{1}{1+\alpha_b\overline{\gamma_{bb}}} \le 1$, and $\frac{\overline{\gamma_{bb}}(1+\overline{\gamma_{mm}})}{\overline{\gamma_{bm}}} < 1$ (from a necessary condition (9) for $r_m(r_b)$ to be concave in any $r_b \in [0, s_b]$ in the proof of Lemma 4.2). ■

For r_b' or r_b'' to be determined with an absolute error ε, it takes at most $\lceil \log(\varepsilon^{-1}) \rceil$ binary search steps. In terms of r_m^*, the error is then less than $1.4\varepsilon\overline{r_b}$, and to find r_m^* with an absolute error ε, the binary search should perform at most $\lceil \log(\varepsilon^{-1} \cdot 1.4\overline{r_b}) \rceil$ steps. ■

To put the number of binary search steps in perspective, the highest SNR typically measured in Wi-Fi and cellular networks is about 50dB (10^5). 50dB SNR maps to $\overline{r_b} \approx 16.61$ b/s/Hz, leading to at most $\lceil 4.53 + \log(\varepsilon^{-1}) \rceil$ binary search steps. As each step requires constant computation, the computation time for determining the TDFD region is very low.

The prof of Theorem 4.7 provides a description of an algorithm for determining the TDFD region, based on all possible cases. Since the pseudocode involves these many different possible cases with relatively simple operations and also due to space constraints, it is deferred to Appendix B in the supplementary material.

Using SC-FD-REGION and SC-TDFD-REGION (App. B), FD and TDFD rate regions were obtained for different combinations of $\overline{\gamma_{bm}}, \overline{\gamma_{mb}}, \overline{\gamma_{mm}}$, and $\overline{\gamma_{bb}}$ (Fig. 7). There are three main observations we can make based on Fig. 7. First, regardless of the XINRs at the MS and BS, as we increase the SNRs, the rate region expands. Second, to see any improvement compared to TDD, the SNRs need to be comparable to or higher than the XINRs. Finally, there are cases when we gain from TDFD but not from FD alone (see, e.g., Fig. 7(d)).

V. MULTI-CHANNEL – FIXED POWER

In this section, we consider the problem of determining FD and TDFD rate regions over multiple channels when the (shape of) the power allocation is fixed, but the total transmission power level can be varied. We first provide characterization of the FD rate region, which allows computing any point on the FD rate region via a binary search. Then, we turn to the problem of determining the TDFD rate region. Due to the lack of structure as in the single channel case, in the multi-channel case the TDFD rate region cannot in general be determined by a binary search. We argue, however, that for inputs that are relevant in practice this problem can be solved in real time.

A. Rate Region

Suppose that we want to determine the FD rate region, given a fixed power allocation over K orthogonal channels: $\alpha_{b,1} = \alpha_{b,2} = ... = \alpha_{b,K} \equiv \alpha_b$ and $\alpha_{m,1} = \alpha_{m,2} = ... = \alpha_{m,K} \equiv \alpha_m$. Note that setting the power allocation so that all $\alpha_{b,k}$'s and all $\alpha_{m,k}$'s are equal is without loss of generality, since we can represent an arbitrary fixed power allocation in this manner by appropriately scaling the values of $\overline{\gamma_{bm,k}}, \overline{\gamma_{mb,k}}, \overline{\gamma_{mm,k}}$, and $\overline{\gamma_{bb,k}}$ (see Eq.'s (16) and (17) below). The sum of the UL and DL rates over the (orthogonal) channels can then be written as $r = r_b + r_m$, where:

$$r_b = \sum_{k=1}^{K} \log\Big(1 + \frac{\alpha_b \overline{\gamma_{bm,k}}}{1 + \alpha_m \overline{\gamma_{mm,k}}}\Big), \text{ and} \tag{16}$$

$$r_m = \sum_{k=1}^{K} \log\Big(1 + \frac{\alpha_m \overline{\gamma_{mb,k}}}{1 + \alpha_b \overline{\gamma_{bb,k}}}\Big). \tag{17}$$

Let $s_b = r_b(\alpha_b = \frac{1}{K}, \alpha_m = \frac{1}{K})$, $s_m = r_m(\alpha_b = \frac{1}{K}, \alpha_m = \frac{1}{K})$. We characterize the FD region in the following lemma.

Lemma 5.1: For a fixed $r_b = r_b^* \leq s_b$, r_m is maximized for $\alpha_m = 1/K$. Similarly, for a fixed $r_m = r_m^* \leq s_m$, r_b is maximized for $\alpha_b = 1/K$.

Proof: We will only prove the first part of the lemma, while the second part will follow using symmetric arguments.

Since r_m is being maximized for a fixed $r_b = r_b^* \leq s_b$, we can think of maximizing r_m by only varying α_m, while α_b changes as a function of α_m to keep $r_b = r_b^*$ as α_m is varied. Observe that for a fixed $\alpha_m \in [0, 1/K]$, α_b such that $r_b = r_b^*$ is uniquely defined since r_b is monotonic in α_b. Because $r_b^* \leq s_b$ and r_b is decreasing in α_m, a solution for α_b such that $r_b = r_b^*$ exists for any $\alpha_m \in [0, 1/K]$. It is not hard to see that $\alpha_b(\alpha_m)$ that keeps $r_b = r_b^*$ is a continuous and differentiable function. This follows from basic calculus, as $\alpha_b(\alpha_m)$ is an inverse function of r_b, and r_b is continuous and strictly increasing in α_b, with $\frac{\partial r_b}{\partial \alpha_b} \neq 0$, $\forall (\alpha_b, \alpha_m) \in [0, 1]^2$. Therefore, we can write:

$$\frac{dr_m(\alpha_m)}{d\alpha_m} = \frac{\partial r_m(\alpha_b, \alpha_m)}{\partial \alpha_m} + \frac{\partial r_m(\alpha_b, \alpha_m)}{\partial \alpha_b} \cdot \frac{d\alpha_b}{d\alpha_m}. \tag{18}$$

From (17), we have:

$$\frac{\partial r_m(\alpha_b, \alpha_m)}{\partial \alpha_m} = \sum_{k=1}^{K} \frac{\overline{\gamma_{mb,k}}}{1 + \alpha_m \overline{\gamma_{mb,k}} + \alpha_b \overline{\gamma_{bb,k}}}, \tag{19}$$

$$\frac{\partial r_m(\alpha_b, \alpha_m)}{\partial \alpha_b} = -\sum_{k=1}^{K} \frac{\frac{\overline{\gamma_{bb,k}}}{1+\alpha_b \overline{\gamma_{bb,k}}} \cdot \alpha_m \overline{\gamma_{mb,k}}}{1 + \alpha_m \overline{\gamma_{mb,k}} + \alpha_b \overline{\gamma_{bb,k}}}. \tag{20}$$

To find $\frac{d\alpha_b}{d\alpha_m}$, we will differentiate $r_b = r_b^*$ (= const.) w.r.t. α_m, using (16):

$$\sum_{k=1}^{K} \frac{\overline{\gamma_{mm,k}} + \overline{\gamma_{bm,k}} \cdot \frac{d\alpha_b}{d\alpha_m}}{1 + \alpha_b \overline{\gamma_{bm,k}} + \alpha_m \overline{\gamma_{mm,k}}} - \sum_{k=1}^{K} \frac{\overline{\gamma_{mm,k}}}{1 + \alpha_m \overline{\gamma_{mm,k}}} = 0$$

$$\begin{aligned} \Leftrightarrow \frac{d\alpha_b}{d\alpha_m} &= \left(\sum_{k=1}^{K} \frac{\overline{\gamma_{bm,k}}}{1 + \alpha_b \overline{\gamma_{bm,k}} + \alpha_m \overline{\gamma_{mm,k}}}\right)^{-1} \\ &\quad \cdot \sum_{k=1}^{K} \frac{\frac{\overline{\gamma_{mm,k}}}{1+\alpha_m \overline{\gamma_{mm,k}}} \cdot \alpha_b \overline{\gamma_{bm,k}}}{1 + \alpha_b \overline{\gamma_{bm,k}} + \alpha_m \overline{\gamma_{mm,k}}} \quad (21) \\ &\leq \alpha_b \cdot \max_{1 \leq j \leq K} \frac{\overline{\gamma_{mm,j}}}{1 + \alpha_m \overline{\gamma_{mm,j}}}. \quad (22) \end{aligned}$$

Plugging (19), (20), and (22) back into (18), we have:

$$\begin{aligned} \frac{dr_m(\alpha_m)}{d\alpha_m} &\geq \sum_{k=1}^{K} \frac{\overline{\gamma_{mb,k}}}{1 + \alpha_m \overline{\gamma_{mb,k}} + \alpha_b \overline{\gamma_{bb,k}}} \\ &- \sum_{k=1}^{K} \frac{\frac{\overline{\gamma_{bb,k}}}{1+\alpha_b \overline{\gamma_{bb,k}}} \cdot \alpha_m \overline{\gamma_{mb,k}}}{1 + \alpha_m \overline{\gamma_{mb,k}} + \alpha_b \overline{\gamma_{bb,k}}} \cdot \max_{1 \leq j \leq K} \frac{\alpha_b \overline{\gamma_{mm,j}}}{1 + \alpha_m \overline{\gamma_{mm,j}}} \\ &= \sum_{k=1}^{K} \frac{\overline{\gamma_{mb,k}}}{1 + \alpha_m \overline{\gamma_{mb,k}} + \alpha_b \overline{\gamma_{bb,k}}} - \max_{1 \leq j \leq K} \frac{\alpha_m \overline{\gamma_{mm,j}}}{1 + \alpha_m \overline{\gamma_{mm,j}}} \\ &\cdot \sum_{k=1}^{K} \frac{\frac{\alpha_b \overline{\gamma_{bb,k}}}{1+\alpha_b \overline{\gamma_{bb,k}}} \cdot \overline{\gamma_{mb,k}}}{1 + \alpha_m \overline{\gamma_{mb,k}} + \alpha_b \overline{\gamma_{bb,k}}} > 0, \end{aligned}$$

where the last inequality follows from $\frac{\alpha_m \overline{\gamma_{mm,j}}}{1+\alpha_m \overline{\gamma_{mm,j}}} < 1$ and $\frac{\alpha_b \overline{\gamma_{bb,k}}}{1+\alpha_b \overline{\gamma_{bb,k}}} < 1$, $\forall j, k$. It follows that r_m is strictly increasing in α_m, and, therefore, maximized for $\alpha_m = 1/K$. ■

We now point out the difference between the proof of Lemma 5.1 and the proof of Theorem 3 in [11]. The proof of Theorem 3 in [11] uses similar arguments as the proof of Lemma 5.1 up to Eq. (18). However, the proof then concludes with the statement that $\frac{\partial r_m}{\partial \alpha_b} < 0$ and $\frac{d\alpha_b}{d\alpha_m} < 0$, which is not correct, as we see from (21) that $\frac{d\alpha_b}{d\alpha_m} > 0$.[5]

[5]In a private communication, the authors of [11] confirmed that our observation was correct and prepared an erratum.

Using Lemma 5.1, we can construct the entire FD rate region by solving (i) $r_b = r_b^*$ for α_b, when $\alpha_m = 1/K$ and $r_b^* \in [0, s_b]$, and (ii) $r_b = r_b^*$ for α_m, when $\alpha_b = 1/K$ and $r_b^* \in (s_b, \overline{r_b}]$. Note that $r_b = r_b^*$ can be solved for α_b when $r_b \in [0, s_b]$ (resp. for α_m) by using a binary search, since r_b is monotonic and bounded in α_b for $r_b \in [0, s_b]$ (resp. α_m for $r_b \in (s_b, \overline{r_b}]$). The pseudocode is provided in Algorithm 3 (MCFIND-r_m). The bound on the running time is provided in Proposition 5.2.

Algorithm 3 MCFIND-$r_m(r_b^*, K)$

```
Input: γ̄_mb, γ̄_bm, γ̄_mm, γ̄_bb
s_b = Σ_{k=1}^{K} log(1 + (1+γ̄_bm/K)/(1+γ̄_mm/K))
if r_b* ≤ s_b then
    Via binary search, find α_b s.t. r_b(α_b, 1/K) = r_b*
    r_m* = Σ_{k=1}^{K} log(1 + (1+γ̄_mb/K)/(1+α_b γ̄_bb))
else
    Via binary search, find α_m s.t. r_b(1/K, α_m) = r_b*
    r_m* = Σ_{k=1}^{K} log(1 + (1+α_m γ̄_mb)/(1+γ̄_bb/K))
return r_m*
```

Proposition 5.2: The running time of MCFIND-r_m is $O(K \log(\sum_k \frac{\overline{\gamma_{bb,k}}}{K\varepsilon}))$, where ε is the additive error for r_m^*.

Proof: To determine α_b with the accuracy ε_α, the binary search takes $\lceil \log({\varepsilon_\alpha}^{-1}/K) \rceil$ steps, as $\alpha_b \in [0, 1/K]$. From (20), we can bound $|\frac{dr_m}{d\alpha_b}|$ as:

$$\Big|\frac{dr_m}{d\alpha_b}\Big| \leq \sum_k \frac{\overline{\gamma_{bb,k}}}{1 + \alpha_b \overline{\gamma_{bb,k}}} \leq \sum_k \overline{\gamma_{bb,k}},$$

as $\frac{\alpha_m \overline{\gamma_{mb,k}}}{1+\alpha_m \overline{\gamma_{mb,k}} + \alpha_b \overline{\gamma_{bb,k}}} \leq 1$, and $1 + \alpha_b \overline{\gamma_{bb,k}} \geq 1, \forall k$. Therefore, to find r_m with the accuracy ε, it suffices to take $\varepsilon = \frac{\varepsilon_\alpha}{\sum_k \overline{\gamma_{bb,k}}}$. As each binary search step takes $O(K)$ computation (due to the computation of $r_b(\alpha_b, 1/K)$), we get the claimed running time bound. ■

Notice that in practice $\overline{\gamma_{bb,k}}/K \leq 1$, $\overline{\gamma_{mm,k}}/K \leq 100$, and K is at the order of 100, which makes the running time of MCFIND-r_m suitable for a real-time implementation.

Unlike in the single channel case, where the shape of the FD region boundary is very structured, in the multi-channel case the region does not necessarily have the property that $r_m(r_b)$ (and $r_b(r_m)$) has at most one concave and one convex piece. To see why this holds, consider the following proposition.

Proposition 5.3: If $r_b \in [0, s_b]$, then

$$\frac{d^2 r_m}{d{r_b}^2} = \Big(\frac{dr_b}{d\alpha_b}\Big)^{-3} \frac{d^2 r_m}{d{\alpha_b}^2} \cdot \frac{dr_b}{d\alpha_b} - \frac{dr_m}{d\alpha_b} \cdot \frac{d^2 r_b}{d{\alpha_b}^2}.$$

Proof: Fix $\alpha_m = 1/K$. As both $r_b(\alpha_b)$ and $\frac{dr_b}{d\alpha_b}$ are increasing and differentiable w.r.t. α_b and $\frac{dr_b}{d\alpha_b} \neq 0$, $\frac{d^2 r_b}{d{\alpha_b}^2} \neq 0$, $\forall \alpha_b \in [0, 1/K]$, it follows that $\alpha_b(r_b)$ is continuous and twice-differentiable w.r.t. r_b. Therefore, we can write:

$$\frac{d^2 r_m}{d{r_b}^2} = \frac{d^2 r_m}{d{\alpha_b}^2} \cdot \left(\frac{d\alpha_b}{dr_b}\right)^2 + \frac{dr_m}{d\alpha_b} \cdot \frac{d^2 \alpha_b}{d{r_b}^2}. \tag{23}$$

From (17), we can determine $\frac{dr_m}{d\alpha_b}$ and $\frac{d^2 r_m}{d{\alpha_b}^2}$:

$$\frac{dr_m}{d\alpha_b} = \sum_{k=1}^{K} \Big(\frac{\overline{\gamma_{bb,k}}}{1 + \alpha_b \overline{\gamma_{bb,k}} + \overline{\gamma_{mb,k}}/K} - \frac{\overline{\gamma_{bb,k}}}{1 + \alpha_b \overline{\gamma_{bb,k}}}\Big),$$

$$\frac{d^2 r_m}{d{\alpha_b}^2} = \sum_{k=1}^{K} \bigg(\Big(\frac{\overline{\gamma_{bb,k}}}{1 + \alpha_b \overline{\gamma_{bb,k}}}\Big)^2 - \Big(\frac{\overline{\gamma_{bb,k}}}{1 + \alpha_b \overline{\gamma_{bb,k}} + \overline{\gamma_{mb,k}}/K}\Big)^2\bigg).$$

To find $\frac{d\alpha_b}{dr_b}$ and $\frac{d^2 \alpha_b}{d{r_b}^2}$, we differentiate (16) w.r.t. r_b to get:

$$\frac{d\alpha_b}{dr_b} = \Big(\frac{dr_b}{d\alpha_b}\Big)^{-1}, \tag{24}$$

$$\frac{d^2 \alpha_b}{d{r_b}^2} = -\left(\frac{dr_b}{d\alpha_b}\right)^{-3} \cdot \frac{d^2 r_b}{d{\alpha_b}^2}. \tag{25}$$

Plugging (24) and (25) back into (23), we have:

$$\frac{d^2 r_m}{d{r_b}^2} = \left(\frac{dr_b}{d\alpha_b}\right)^{-3} \left(\frac{d^2 r_m}{d{\alpha_b}^2} \cdot \frac{dr_b}{d\alpha_b} - \frac{dr_m}{d\alpha_b} \cdot \frac{d^2 r_b}{d{\alpha_b}^2}\right).$$

■

From Proposition 5.3, as $\left(\frac{dr_b}{d\alpha_b}\right)^{-3} > 0$, the sign of $\frac{d^2 r_m}{d{r_b}^2}$ is determined by the sign of $\frac{d^2 r_m}{d{\alpha_b}^2} \cdot \frac{dr_b}{d\alpha_b} - \frac{dr_m}{d\alpha_b} \cdot \frac{d^2 r_b}{d{\alpha_b}^2}$, which can be equivalently written as a rational function of α_b with linear-in-K degree of the polynomial in its numerator. Therefore, the number of roots of $\frac{d^2 r_m}{d{r_b}^2}$ can be linear in K, and so r_m can have up to linear in K concave and convex pieces. When $K = 1$, $\frac{d^2 r_m}{d{\alpha_b}^2} \cdot \frac{dr_b}{d\alpha_b} - \frac{dr_m}{d\alpha_b} \cdot \frac{d^2 r_b}{d{\alpha_b}^2}$ can be factored as:

$$\frac{\overline{\gamma_{bm}}}{1 + \alpha_b \overline{\gamma_{bm}} + \overline{\gamma_{mm}}} \cdot \Big(\frac{\overline{\gamma_{bb}}}{1 + \alpha_b \overline{\gamma_{bb}} + \overline{\gamma_{mb}}} - \frac{\overline{\gamma_{bb}}}{1 + \alpha_b \overline{\gamma_{bb}}}\Big)$$
$$\cdot \Big(\frac{\overline{\gamma_{bb}}}{1 + \alpha_b \overline{\gamma_{bb}} + \overline{\gamma_{mb}}} + \frac{\overline{\gamma_{bb}}}{1 + \alpha_b \overline{\gamma_{bb}}} - \frac{\overline{\gamma_{bm}}}{1 + \alpha_b \overline{\gamma_{bm}} + \overline{\gamma_{mm}}}\Big).$$

Simplifying the rational expressions in $\Big(\frac{\overline{\gamma_{bb}}}{1+\alpha_b \overline{\gamma_{bb}} + \overline{\gamma_{mb}}} + \frac{\overline{\gamma_{bb}}}{1+\alpha_b \overline{\gamma_{bb}}} - \frac{\overline{\gamma_{bm}}}{1+\alpha_b \overline{\gamma_{bm}} + \overline{\gamma_{mm}}}\Big)$, we can recover the same quadratic function in the numerator as we had in (10) and yield the same conclusions as in Lemma 4.2, since $\frac{\overline{\gamma_{bm}}}{1+\alpha_b \overline{\gamma_{bm}} + \overline{\gamma_{mm}}} \cdot \Big(\frac{\overline{\gamma_{bb}}}{1+\alpha_b \overline{\gamma_{bb}} + \overline{\gamma_{mb}}} - \frac{\overline{\gamma_{bb}}}{1+\alpha_b \overline{\gamma_{bb}}}\Big) > 0$. However, there does not seem to be a direct extension of this result to the $K > 1$ case.

Although in general the problem of convexifying the FD region seems difficult in the multi-channel case, in practice it can be solved efficiently. The reason is that in Wi-Fi and cellular networks the output power levels take values from a discrete set of size N, where $N < 100$. Therefore, (for fixed $\overline{\gamma_{mb,k}}$, $\overline{\gamma_{bm,k}}$, $\overline{\gamma_{bb,k}}$, $\overline{\gamma_{mm,k}}$, $\forall k$) r_b can take at most N distinct values. To find the TDFD rate region, since the points of the FD region are determined in order increasing in r_b, $\Theta(N)$ computation suffices (Ch. 33, [21]).

The rate regions and the rate improvements for $\overline{\gamma_{bb,k}}$ described by Fig. 2(a) and the three cases of $\overline{\gamma_{mm,k}}$ described by Fig. 2(b)–(d), for equal power allocation and equal SNR over channels, are shown in Figs. 9 and 10, respectively. As the cancellation becomes more broadband, namely as $\overline{\gamma_{mm,k}}$'s change from those described in Fig. 2(b) over 2(c) to 2(d), the rate improvements become higher and the rate region becomes convex for lower values of $\overline{\gamma_{mb}}$ and $\overline{\gamma_{bm}}$.

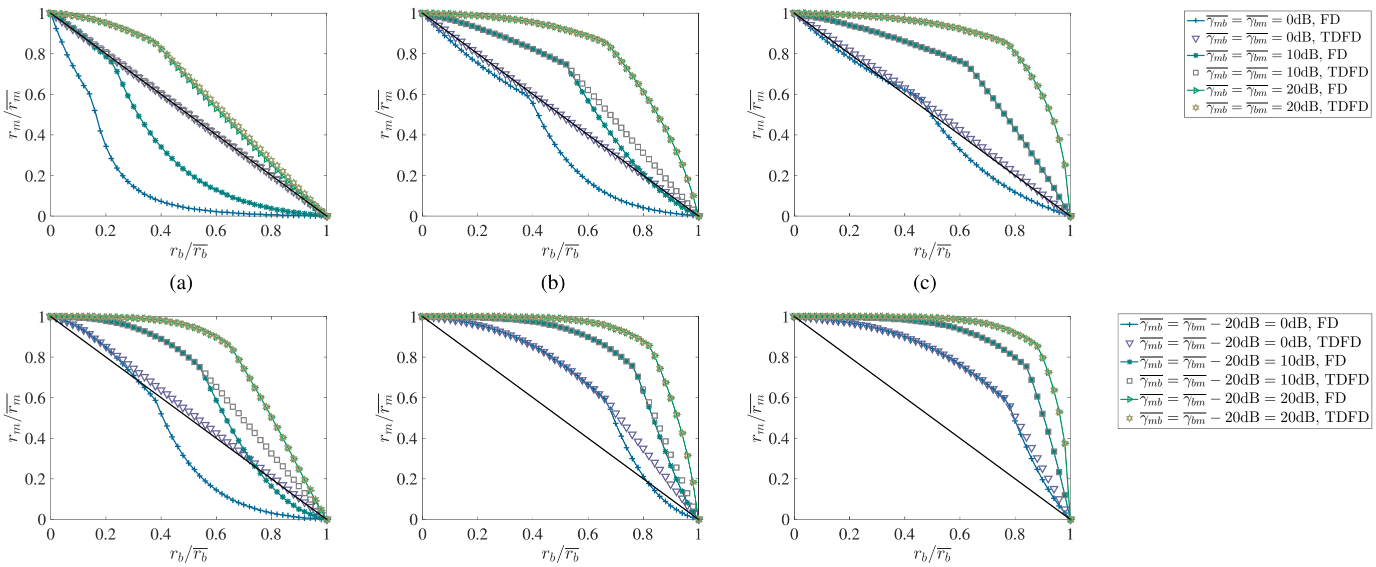

(a) (b) (c)

(d) (e) (f)

Fig. 9: Rate regions for $\overline{\gamma_{bb,k}}$ from Fig. 2(a), and $\overline{\gamma_{mm,k}}$ from (a), (d) Fig. 2(b); (b), (e) Fig. 2(c); and (c), (f) Fig. 2(d).

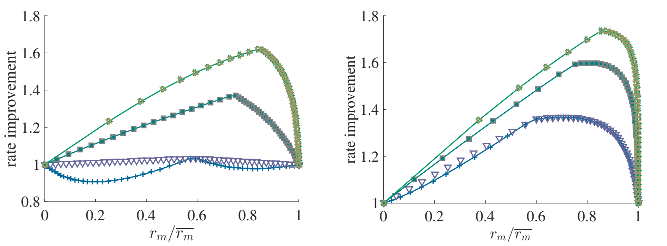

(a) (b)

Fig. 10: Rate improvements corresponding to rate regions from (a) Fig. 9(c) and (b) Fig. 9(f).

VI. Multi-Channel – General Power

We now consider the computation of TDFD rate regions under general power allocations. In this case there are $2K$ variables ($\alpha_{b,1}, ..., \alpha_{b,K}$, $\alpha_{m,1}, ..., \alpha_{m,K}$), compared to 2 variables (α_b and α_m) from the previous section.

Computing $r_m^* = \max\{r_m : r_b = r_b^*\}$ is a non-convex problem, and is hard to optimize in general. Yet, we present an algorithm that is guaranteed to converge to a stationary point, under certain restrictions. In practice, the stationary point to which it converges is also a global maximum. The restrictions are based on [13] and they guarantee that $r_b + r_m$ is concave when either the $\alpha_{b,k}$'s or $\alpha_{m,k}$'s are fixed. Note that the restrictions do not make the problem $r_m^* = \max\{r_m : r_b = r_b^*\}$ convex (see Section VI-A). The restrictions are mild in the sense that they do not affect the optimum by much whenever $\overline{\gamma_{bm,k}}$ and $\overline{\gamma_{mb,k}}$ do not differ much.

Though for many practical cases the algorithm is near-optimal and runs in polynomial time, its running time in general is not suitable for a real-time implementation. To combat the high running time, in Section VI-B we develop a simple heuristic that in most cases has similar performance.

A. Rate Region

Determining the FD region under a general power allocation is equivalent to solving $\{\max r_m : r_b = r_b^*\}$ for any $r_b^* \in [0, \overline{r_b}]$ over $\alpha_{b,k}, \alpha_{m,k} \geq 0$, $\sum_k \alpha_{b,k} \leq 1$, $\sum_k \alpha_{m,k} \leq 1$. It is not hard to show that $\frac{dr_m}{dr_b} < 0$, and, therefore, the problem is equivalent to $(P) = \{\max r_m : r_b \geq r_b^*\}$.

Problem (P) is not convex, even when some of the variables are fixed. When the $\alpha_{m,k}$'s are fixed, r_b is concave in $\alpha_{b,k}$'s and the feasible region is convex, however, r_m is convex as well. Conversely, when the $\alpha_{b,k}$'s are fixed, r_m is concave in $\alpha_{m,k}$'s, but the feasible region is not convex since r_b is convex in $\alpha_{m,k}$'s. Therefore, the natural approach to determining the FD region fails.

On the other hand, [13] provides conditions that guarantee that $\forall k$, $r = r_b + r_m$ is (i) concave and increasing in $\alpha_{m,k}$ when $\alpha_{b,k}$ is fixed, and (ii) concave and increasing in $\alpha_{b,k}$ when $\alpha_{m,k}$ is fixed. These conditions are not very restrictive: when they cannot be satisfied, one cannot gain much from FD additively – the additive gain is less than 1b/s/Hz compared to the maximum of the UL and DL rates. However, these conditions can be very restrictive when the difference between $\overline{r_b}$ and $\overline{r_m}$ is high. The conditions are:

$$\overline{\gamma_{bm,k}} \geq \overline{\gamma_{bb,k}}(1 + \alpha_{m,k}\overline{\gamma_{mm,k}}), \forall k \tag{C1}$$

$$\overline{\gamma_{mb,k}} \geq \overline{\gamma_{mm,k}}(1 + \alpha_{b,k}\overline{\gamma_{bb,k}}), \forall k. \tag{C2}$$

Notice that when $\overline{\gamma_{bm,k}} \geq \overline{\gamma_{bb,k}}(1 + \overline{\gamma_{mm,k}})$ and $\overline{\gamma_{mb,k}} \geq \overline{\gamma_{mm,k}}(1 + \overline{\gamma_{bb,k}})$, conditions (C1) and (C2) are non-restrictive (as they hold for any $\alpha_{b,k} \leq 1$, $\alpha_{mk} \leq 1$). When $\overline{\gamma_{bm,k}} < \overline{\gamma_{bb,k}}$, (C1) cannot be satisfied for any $\alpha_{m,k}$ as $\alpha_{m,k} \geq 0$. Similarly for $\overline{\gamma_{mb,k}} < \overline{\gamma_{mm,k}}$, (C2) cannot hold for any $\alpha_{b,k}$.

We will use conditions (C1) and (C2) to formulate a new problem that is still non-convex, but more tractable than the original problem (P). This way, we will get an upper bound on the rate region and rate improvements when the conditions are non-restrictive. The new problem will also allow us to make a good estimate of the rate region in the cases when $\overline{\gamma_{bm,k}}$ and $\overline{\gamma_{mb,k}}$ do not differ much.

Let (s_b, s_m) denote the UL-DL rate pair that maximizes the sum of the rates over UL and DL channels.

Lemma 6.1: If conditions (C1) and (C2) are non-restrictive, then, given $\overline{\gamma_{bm,k}}, \overline{\gamma_{mb,k}}, \overline{\gamma_{mm,k}}, \overline{\gamma_{bb,k}}$ for $k \in \{1, ..., K\}$, the TDFD rate region can be determined by solving:

$$(Q) = \begin{cases} \max & \sum_{k=1}^{K}(r_{b,k}(\alpha_{b,k}, \alpha_{m,k}) + r_{m,k}(\alpha_{b,k}, \alpha_{m,k})) \\ \text{s.t.} & \sum_{k=1}^{K} r_{b,k}(\alpha_{b,k}, \alpha_{m,k}) \text{ op } r_b^* \\ & \sum_{k=1}^{K} \alpha_{b,k} \leq 1, \sum_{k=1}^{K} \alpha_{m,k} \leq 1 \\ & \alpha_{b,k} \geq 0, \alpha_{m,k} \geq 0, \forall k \end{cases},$$

where op $='\leq'$, if $r_b^* \leq s_b$ and op $='\geq'$, if $r_b^* \geq s_b$.

Proof: First, observe that if we had op $='='$, then (Q) would be equivalent to (P). Therefore, if an optimal solution to (Q) satisfies $r_b = r_b^*$, then it also optimally solves (P).

Suppose that $r_b^* \leq s_b$ and that an optimal solution (r_b^Q, r_m^Q) to (Q) satisfies $r_b^Q < r_b^*$. Let (r_b^P, r_m^P), where $r_b^P = r_b^*$, be the optimal solution to (P). Observe that $r_b^P + r_m^P \leq r_b^Q + r_m^Q$, and, as $r_b^Q < r_b^* = r_b^P$, it also holds that $r_m^Q > r_m^P$. Let $\lambda \in (0, 1)$ be the solution to $r_b^* = \lambda r_b^Q + (1-\lambda)s_b$ (such a λ exists and is unique as $r_b < s_b$). Then, as $s_b + s_m \geq r_b^P + r_m^P$ and $r_b^Q + r_m^Q \geq r_b^P + r_m^P$, we have:

$$\begin{aligned} \lambda(r_b^Q + r_m^Q) + (1-\lambda)(s_b + s_m) &= r_b^P + \lambda r_m^Q + (1-\lambda)s_m \\ &\geq r_b^P + r_m^P, \end{aligned}$$

and we have $\lambda r_m^Q + (1-\lambda)s_m \geq r_m^P$. Therefore, we can get a point (r_b^*, r_m) with $r_m \geq r_m^P$ as a convex combination of the points that optimally solve both (P) and (Q). In other words, the convex hull of the points determined by (Q) is the TDFD rate region. To find the convex hull of the points determined by (Q), we can employ an algorithm for finding a convex hull of given points from e.g., [21].

A similar argument follows for $r_b^* > s_b$. ■

When conditions (C1) and (C2) are restrictive, they provide upper bounds on $\alpha_{b,k}$ and $\alpha_{m,k}$ and they do not affect the optimal solution to (Q) unless $\overline{\gamma_{bm,k}} >> \overline{\gamma_{mb,k}}$ or $\overline{\gamma_{mb,k}} >> \overline{\gamma_{bm,k}}$ for some k. To avoid infeasibility when restricting the feasible region of (Q) by requiring (C1) and (C2), similar to [13], we will set either $\alpha_{b,k} = 0$ or $\alpha_{m,k} = 0$.[6]

We write the restrictions imposed by (C1) and (C2) on the feasible region of (Q) as follows, where $\alpha_{b,k} \leq A_b(k)$ and $\alpha_{m,k} \leq A_m(k)$, $\forall k$. Notice that the restrictions are fixed for fixed $\overline{\gamma_{bm,k}}, \overline{\gamma_{mb,k}}, \overline{\gamma_{mm,k}}, \overline{\gamma_{bb,k}}$, and r_b^*. We refer to the restricted version of problem (Q) as (Q_R).

To solve (Q_R), we will use a well-known practical method called alternating minimization (or maximization, as in our case) [22]. For a given problem (P_i), the method partitions the set of variables x into two sets x_1 and x_2, and then iteratively applies the following procedure: (i) optimize (P_i) over x_1 by treating the variables from x_2 as constants, (ii) optimize (P_i) over x_2 by treating the variables from x_1 as constants, until a stopping criterion is reached.

[6]Recall that when $\alpha_{b,k} = 0$, the sum of the rates is concave in $\alpha_{m,k}$ for any $\alpha_{m,k} \in [0, 1]$. Similarly when $\alpha_{m,k} = 0$.

Algorithm 4 DETERMINE-Q_R

```
Input: {γ̄_bb,k}, {γ̄_mm,k}, {γ̄_mb,k}, {γ̄_bm,k}, r_b*
Let A_b and A_m be size-K arrays
for k = 1 to K do
    A_b(k) = (γ̄_mb,k/γ̄_mm,k − 1)/γ̄_bb,k,  A_m(k) = (γ̄_bm,k/γ̄_bb,k − 1)/γ̄_mm,k
    if r_b* ≤ s_b then
        if A_b(k) ≤ 0 then A_b(k) = 0, A_m(k) = 1
        if A_m(k) ≤ 0 then A_m(k) = 0, A_b(k) = 1
    else
        if A_m(k) ≤ 0 then A_m(k) = 0, A_b(k) = 1
        if A_b(k) ≤ 0 then A_b(k) = 0, A_m(k) = 1
return (Q_R) = (A_m, A_b)
```

Even in the cases when (P_i) is non-convex, if subproblems from (i) and (ii) have unique solutions and are solved optimally in each iteration, the method converges to a stationary point with rate $O(1/\sqrt{n})$, where n is the iteration count [23]. In the cases when, in addition, for each of the subproblems the objective is convex (concave for maximization problems), for each stationary point there exists an initial point such that the alternating minimization converges to that stationary point [24]. A common approach that works well in practice is to generate many random initial points and choose the best solution found. In our experiments, choosing $\alpha_{b,k} = \alpha_{m,k} = 0$ as the initial point typically led to the best solution.

Due to the added restrictions in problem (Q_R) imposed by (C1) and (C2), the objective in (Q_R) is concave whenever either all $\alpha_{b,k}$'s or all $\alpha_{m,k}$'s are fixed, while the remaining variables are varied. Hence, our two subproblems for Q_R will be: (i) $(Q_{R,b})$, which is equivalent to (Q_R) except that it treats $\alpha_{b,k}$'s as variables and $\alpha_{m,k}$'s as constants, and (ii) $(Q_{R,m})$, which is equivalent to (Q_R) except that it treats $\alpha_{m,k}$'s as variables and $\alpha_{b,k}$'s as constants. Given accuracy ε, the pseudocode is provided in Algorithm 5 (ALTMAX). The rate pair (s_b, s_m) can be determined using the same algorithm by omitting the constraint $r_b \leq r_b^*$ (or $r_b \geq r_b^*$).

Algorithm 5 ALTMAX$((Q_R), \varepsilon)$

```
Let {α⁰_b,k}, {α⁰_m,k} be a feasible solution to (Q_R), n = 0
repeat
    n = n + 1
    {αⁿ_b,k} = arg max{(Q_R,b) : {αⁿ_m,k} = {αⁿ⁻¹_m,k}}
    {αⁿ_m,k} = arg max{(Q_R,m) : {αⁿ_b,k} = {αⁿ⁻¹_b,k}}
until max_k{|αⁿ_b,k − αⁿ⁻¹_b,k| + |αⁿ_m,k − αⁿ⁻¹_m,k|} < ε
```

What remains to show is that both $(Q_{R,b})$ and $(Q_{R,m})$ have unique solutions that can be found in polynomial time. We do that in the following (constructive) lemma. Note that without the constraint $r_b^* \leq s_b$ or $r_b^* \geq s_b$, both $(Q_{R,b})$ and $(Q_{R,m})$ are convex and have strictly concave objectives, and therefore, we can determine s_b using ALTMAX.

Lemma 6.2: Starting with a feasible solution $\{\alpha_{b,k}^0, \alpha_{m,k}^0\}$ to (Q_R), in each iteration of ALTMAX the solutions to $(Q_{R,b})$ and $(Q_{R,m})$ are unique and can be found in polynomial time.

Proof: Suppose that $r_b^* \leq s_b$. Then it is not hard to verify that $(Q_{R,m})$ is a convex problem with a strictly concave objective. The objective is strictly concave due to the enforcement of conditions (C1) and (C2), while all the constraints except for $r_b \leq r_b^*$ are linear. The constraint $r_b \leq r_b^*$ is convex as r_b is convex in $\alpha_{m,k}$'s. Therefore, $(Q_{R,m})$ admits a unique solution that can be found in polynomial time through convex programming. By similar arguments, when $r_b^* > s_b$, $(Q_{R,b})$ admits a unique solution that can be found in polynomial time through convex programming.

Consider $(Q_{R,b})$ when $r_b^* \leq s_b$. This problem is not convex due to the constraint $r_b \leq r_b^*$, as r_b is concave in $\alpha_{b,k}$'s. However, we will show that the problem has enough structure so that it is solvable in polynomial time.

Let $k^* = \arg\max_k \left\{ \frac{\overline{\gamma_{bm,k}}}{1+\alpha_{m,k}\overline{\gamma_{mm,k}}} - \overline{\gamma_{bb,k}} + \frac{\overline{\gamma_{bb,k}}}{1+\alpha_{m,k}\overline{\gamma_{mb,k}}} \right\}$ $(= \arg\max_k \left\{ \frac{dr}{d\alpha_{b,k}}\Big|_{\alpha_{b,k}=0} \right\})$. Recall that, due to conditions (C1) and (C2), we have that $\frac{d^2 r}{d\alpha_{b,k}{}^2} < 0$, and therefore $\frac{dr}{d\alpha_{b,k}}$ is monotonically decreasing, $\forall k$. It follows that for any $\alpha_{b,k^*} \in [0,1]$ and any $k \in \{1, ..., K\}$, either there exists a (unique) $\alpha_{b,k} \in [0,1]$ such that $\frac{dr}{d\alpha_{b,k}} = \frac{dr}{d\alpha_{b,k^*}}$, or $\frac{dr}{d\alpha_{b,k}} < \frac{dr}{d\alpha_{b,k^*}}$, $\forall \alpha_{b,k} \in [0,1]$.

Consider Algorithm 6 (SOLVESUBPROBLEMb) and let $\{\alpha_{b,k}^*\}$ be the solution returned by the algorithm. Note that the binary search for finding α_{b,k^*}^* and for determining $\alpha_{b,k}^*$'s in SOLVESUBPROBLEMb is correct from the choice of k^* and because $\frac{dr}{d\alpha_{b,k}}$ is monotonically decreasing, $\forall k$.

Algorithm 6 SOLVESUBPROBLEMb

```
k* = argmax_k { γ̄_bm,k/(1+α_m,k γ̄_mm,k) − γ̄_bb,k + γ̄_bb,k/(1+α_m,k γ̄_mb,k) }
For α_b,k* ∈ [0,1], via binary search, find the maximum α_b,k*
   such that r_b ≤ r_b* and Σ_k α_b,k ≤ 1, where:
if dr/dα_b,k |_(α_b,k=0) < dr/dα_b,k* then α_b,k = 0
else
    Via binary search over α_b,k ∈ [0,1], find α_b,k such that
    dr/dα_b,k = dr/dα_b,k*
```

We first show that $\{\alpha_{b,k}^*\}$ is a local maximum for (Q_b). Because of the algorithm's termination conditions, it must be either $\sum_k \alpha_{b,k}^* = 1$ or $r_b = r_b^*$. If $\sum_k \alpha_{b,k}^* = 1$, then to move to any alternative solution, the total change must be $\sum_k \Delta\alpha_{b,k} \leq 0$, or, equivalently $\Delta\alpha_{b,k^*} \leq -\sum_{k \neq k^*} \Delta\alpha_{b,k}$. As $\frac{dr}{d\alpha_{b,k}} \leq \frac{dr}{d\alpha_{b,k^*}}$, it follows that $\sum_k \frac{dr}{d\alpha_{b,k}} \Delta\alpha_{b,k} \leq 0$, which is the first-order optimality condition. Now suppose that $r_b = r_b^*$. Since $\frac{dr}{d\alpha_{b,k}} = \frac{dr_b}{d\alpha_{b,k}} + \frac{dr_m}{d\alpha_{b,k}} > 0$ and $\frac{dr_b}{d\alpha_{b,k}} > 0$, $\frac{dr_m}{d\alpha_{b,k}} < 0$, to keep the solution feasible (i.e., to keep $r_b \leq r_b^*$), we must have $\sum_k \frac{dr_{b,k}}{d\alpha_{b,k}} \Delta\alpha_{b,k} \leq 0$, which implies $\sum_k \frac{dr}{d\alpha_{b,k}} \Delta\alpha_{b,k} \leq 0$. Therefore, $\{\alpha_{b,k}^*\}$ computed by SOLVESUBPROBLEMb is a local optimum.

In fact, for any local optimum: $\frac{dr}{d\alpha_{b,k}} \leq \frac{dr}{d\alpha_{b,k^*}}$, otherwise we can construct a better solution. Suppose that $\frac{dr}{d\alpha_{b,j}} > \frac{dr}{d\alpha_{b,k^*}}$ for some j. Then if $\frac{dr_b}{d\alpha_{b,j}} \leq \frac{dr_b}{d\alpha_{b,k^*}}$, we can choose a sufficiently small $\Delta > 0$, so that the solution $\{\alpha'_{b,k}\}$ with $\alpha'_{b,j} = \alpha_{b,j} + \Delta$, $\alpha'_{b,k^*} = \alpha_{b,k^*} - \Delta$, and $\alpha'_{b,k} = \alpha_{b,k}$ for $k \notin \{j, k^*\}$ is feasible. For such a solution $\sum_k \frac{dr}{d\alpha_{b,k}}(\alpha'_{b,k} - \alpha_{b,k}) > 0$, and therefore, it is not a local optimum. Conversely, if $\frac{dr_b}{d\alpha_{b,j}} > \frac{dr_b}{d\alpha_{b,k^*}}$, we can choose sufficiently small $\Delta_1, \Delta_2 > 0$ such that $\Delta_2 > \Delta_1$ and $\frac{dr}{d\alpha_{b,j}} \Delta_1 > \frac{dr}{d\alpha_{b,k^*}} \Delta_2$. Then, we can construct an $\{\alpha'_{b,k}\}$ with $\alpha'_{b,j} = \alpha_{b,j} + \Delta_1$, $\alpha'_{b,k^*} = \alpha_{b,k^*} - \Delta_2$, and $\alpha'_{b,k} = \alpha_{b,k}$ for $k \notin \{j, k^*\}$ that is feasible. Again, we have $\sum_k \frac{dr}{d\alpha_{b,k}}(\alpha'_{b,k} - \alpha_{b,k}) > 0$, and $\{\alpha_{b,k}\}$ cannot be a local maximum.

Finally, since $\{\alpha_{b,k}^*\}$ returned by SOLVESUBPROBLEMb satisfies $\alpha_{b,k}^* \geq \alpha'_{b,k}$ for any other local maximum $\{\alpha'_{b,k}\}$ and the objective is strictly increasing in all $\alpha_{b,k}$'s, $\{\alpha_{b,k}^*\}$ must be a global maximum. From the strict monotonicity of $\frac{dr}{d\alpha_{b,k}}$, this maximum is unique. The proof for $(Q_{R,m})$ when $r_b^* \geq s_b$ uses similar arguments and is omitted. ■

B. A Simple Power Allocation Heuristic

Even though the algorithm described in the previous section leads to the optimal or a near-optimal TDFD rate region in many cases of interest, it may not be suitable for a real-time implementation. This motivates us to develop a simple heuristic that performs well in most cases and is based on the observations we made while implementing the algorithms described in previous sections.

Algorithm 7 PA-HEURISTIC(K, r_b^*)

```
Input: {γ̄_bm,k, γ̄_mb,k, γ̄_mm,k, γ̄_bb,k}
{α^L_b,k} = arg{r̄_b}, {α^L_m,k} = arg{r̄_m}
{α^H_b,k}, {α^H_m,k} = arg{s_b + s_m}
f_1 = true, f_2 = true, k = 1
if r_b* ≤ s_b then
    j = 0, {α^1_b,k} = {α^L_b,k}, {α^2_b,k} = {α^H_b,k}
    while j ≤ K/2 and (f_1 or f_2) do
        {γ̄^1_bm,k, γ̄^1_mb,k, γ̄^1_mm,k, γ̄^1_bb,k} = SCALE({α^1_b,k, α^L_m,k})
        r^1_m = MCFIND-r_m(r_b*, K) for input above
        {γ̄^2_bm,k, γ̄^2_mb,k, γ̄^2_mm,k, γ̄^2_bb,k} = SCALE({α^2_b,k, α^H_m,k})
        r^2_m = MCFIND-r_m(r_b*, K) for input above
        if j = 0 then
            r_m* = max{r^1_m, r^2_m}
        else
            {α^t_b,k} = {α^1_b,k}/(Σ_k α^1_b,k), α^t_b,j = 0
            if r_b({α^t_b,k}, {α^L_m,k}) ≥ r_b* and MCFIND-r_m(r_b*, K) >
              r_m* with input = {γ̄^1_bm,k, γ̄^1_mb,k, γ̄^1_mm,k, γ̄^1_bb,k}
            then
                r_m* = MCFIND-r_m(r_b*, K), {α^1_b,k} = {α^t_b,k}
            else f_1 = false
            {α^t_b,k} = {α^2_b,k}/(Σ_k α^2_b,k), α^t_b,K−j+1 = 0
            if r_b({α^t_b,k}, {α^L_m,k}) ≥ r_b* and MCFIND-r_m(r_b*, K) >
              r_m* with input = {γ̄^2_bm,k, γ̄^2_mb,k, γ̄^2_mm,k, γ̄^2_bb,k}
            then
                r_m* = MCFIND-r_m(r_b*, K), {α^2_b,k} = {α^t_b,k}
            else f_2 = false
            j = j + 1
else
    Use a similar procedure as for r_b* ≤ s_b.
```

Algorithm 8 SCALE$(\{\alpha_{b,k}, \alpha_{m,k}\})$

```
Input: {γ̄_bm,k, γ̄_mb,k, γ̄_mm,k, γ̄_bb,k}
for k = 1 to K do
    γ̄_bm,k^s = K α_b,k γ̄_bm,k,  γ̄_mb,k^s = K α_m,k γ̄_mb,k
    γ̄_mm,k^s = K α_m,k γ̄_mm,k,  γ̄_bb,k^s = K α_b,k γ̄_bb,k
return {γ̄_bm,k^s, γ̄_mb,k^s, γ̄_mm,k^s, γ̄_bb,k^s}
```

The intuition for the heuristic is that around the points $(0, \overline{r_m})$ and $(\overline{r_b}, 0)$, one of the two rates is very low, and the power allocation at the station with the high rate behaves as the optimal HD power allocation. When the SNR on each channel

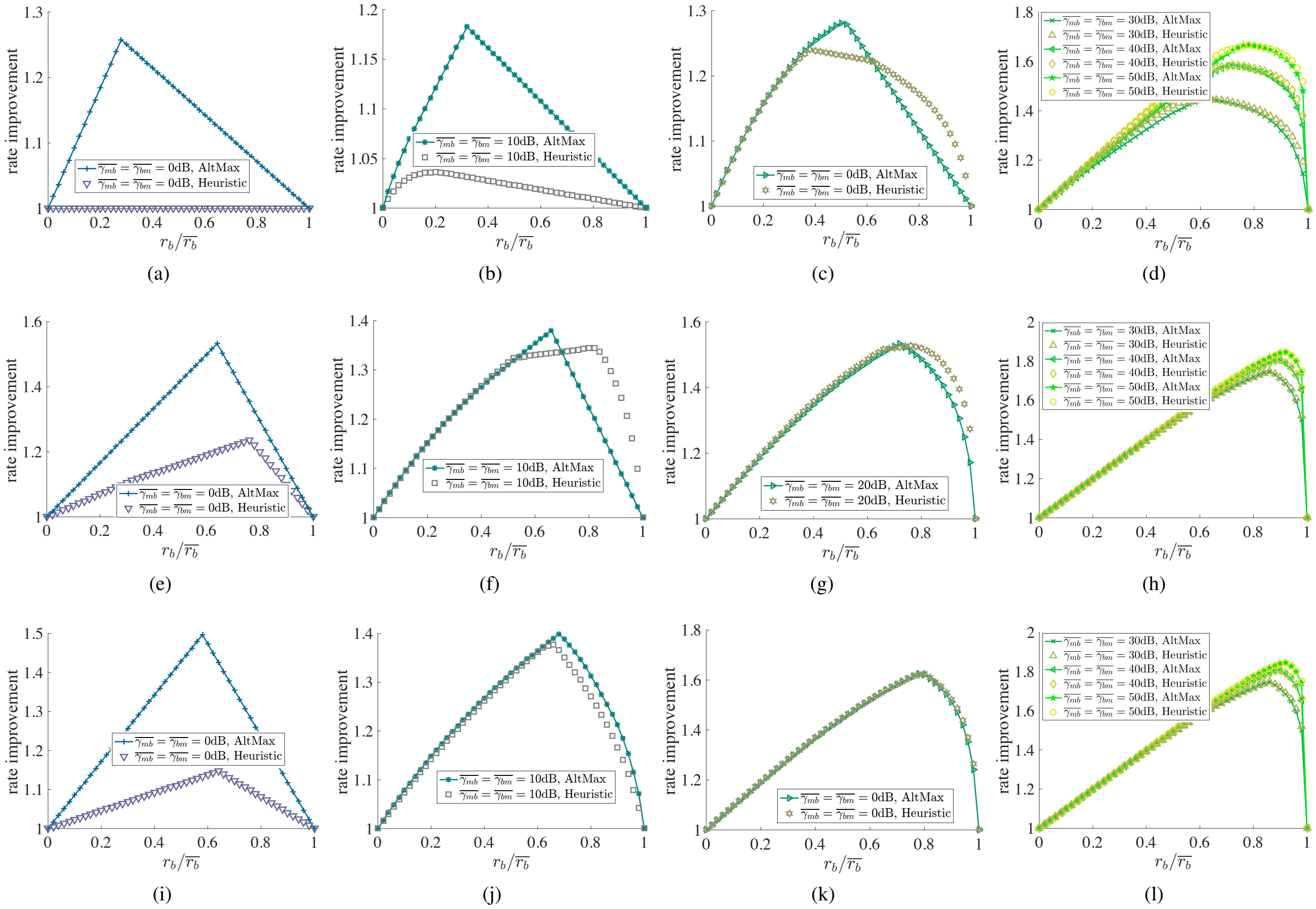

Fig. 11: Comparison of rate improvements for rate regions computed by AltMax and the heuristic. XINR at the BS in all the plots is assumed to be as in Fig.2(a). The XINR at the MS is as in: (i) 2(b) for the graphs in the first row, (ii) 2(c) for the graphs in the second row, and (iii) 2(d) for the graphs in the third row.

and at both stations is high compared to the XINR, the power allocation around the point (s_b, s_m) has the shape of the power allocation in the high SINR approximation[7]. When the SNR compared to the XINR is high on some channels, but not high on the other channels, then it may be better to use some of the channels with low SNR as HD. For practical implementations of compact FD transceivers, the channels with the higher XINR typically appear closer to the edges of the frequency band. The pseudocode of the heuristic for the case $r_b^* \leq s_b$ is provided in Algorithm 7 (PA-HEURISTIC). The pseudocode for $r_b^* > s_b$ is analogous to the $r_b^* \leq s_b$ case and is omitted. Here, (s_b, s_m) is obtained as the rate pair that maximizes the sum rate under the high SINR approximation, as in [13].

For the FD rate region determined by the heuristic, we further run a convex hull computation algorithm [21] to determine the TDFD rate region. The total running time is $O(NK^2 \log(\sum_k \overline{\gamma_{bb,k}}/(K\varepsilon)))$ for computing N points on the FD rate region boundary by using PA-HEURISTIC, plus additional $O(N)$ for convexifying the rate region. Note that in practice K and N are at the order of 100, which makes this algorithm real-time.

The comparison of the rate improvement for TDFD operation determined by PA-HEURISTIC and the alternating maximization algorithm described in the previous section is shown in Fig. 11. The results shown in Fig. 11 were obtained assuming that $\overline{\gamma_{bm,1}} = \overline{\gamma_{bm,K}} \dots \equiv K\overline{\gamma_{bm}}$, $\overline{\gamma_{mb,1}} = \dots = \overline{\gamma_{mb,K}} \equiv K\overline{\gamma_{mb}}$, and $\overline{\gamma_{mm,k}}, \overline{\gamma_{bb,k}}$ from Fig. 2. The alternating maximization algorithm can provide an optimal solution only when conditions (C1) and (C2) are non-restrictive, i.e., when $\overline{\gamma_{bm,k}} \geq \overline{\gamma_{bb,k}}(1+\overline{\gamma_{mm,k}})$ and $\overline{\gamma_{mb,k}} \geq \overline{\gamma_{mm,k}}(1+\overline{\gamma_{bb,k}})$, $\forall k$. For $\overline{\gamma_{bb,k}}$ from Fig. 2(a) and $\overline{\gamma_{mm,k}}$ from Fig. 2(b), (c), and (d), (C1) and (C2) are non-restrictive when (i) $\overline{\gamma_{bm}} \geq 39.1$dB, $\overline{\gamma_{mb}} \geq 39.2$dB, (ii) $\overline{\gamma_{bm}} \geq 32.8$dB, $\overline{\gamma_{mb}} \geq 32.3$dB, and (iii) $\overline{\gamma_{bm}} \geq 25.3$dB, $\overline{\gamma_{mb}} \geq 25.3$dB, respectively.

Results in Fig. 11 are organized as follows. The first row corresponds to the XINR profile $\overline{\gamma_{mm,k}}$ at the MS as in Fig. 2(b) (narrowband canceller), the second row corresponds to the XINR profile $\overline{\gamma_{mm,k}}$ at the MS as in Fig. 2(c) (medium-band canceller), and the third row corresponds to the XINR profile $\overline{\gamma_{mm,k}}$ at the MS as in Fig. 2(d) (wideband canceller). Going from the left-most column to the right, the average SNR $\overline{\gamma_{mb}} = \overline{\gamma_{bm}}$ is increased in 10dB steps, starting from

[7]See [13] for the high SINR approximation power allocation.

0dB in the left-most-column, and ending with $\overline{\gamma_{mb}} = \overline{\gamma_{bm}} \in \{30, 40, 50\}$dB in the right-most column.

When the average SNR is low compared to the XINR, the heuristic cannot lead to high rate improvements. However, we can still observe significant gains from ALTMAX (the left-most column in Fig. 11). What happens in this case is that ALTMAX obtains high rate improvements not from using full-duplex, but from the higher total transmission power at the MS and the BS – this was also observed for the maximization of the sum of the rates in [13]. As the average SNR increases (moving from left to right in Fig. 11), the effect of the higher total transmission power becomes lower and we can see that when the maximum rate improvement is over 40%, PA-HEURISTIC and ALTMAX provide very similar results. In particular, when the average SNR is high (the right-most column in Fig. 11), the two algorithms provide almost indistinguishable results.

VII. CONCLUSION

We presented a theoretical study of the rate region of FD in both the single and multi-channel cases. We developed algorithms that not only allow characterizing the region but can also be used for asymmetrical rate allocation. We numerically demonstrated the gains from FD. While significant attention has been given to resource allocation in HD OFDM networks (e.g., [25] and references therein), as we demonstrated, the special characteristics of FD pose many new challenges. In particular, the design of MAC protocols that support the co-existence of HD and FD users while providing fairness is an open problem. Moreover, there is a need for experimental evaluation of scheduling, power control, and channel allocation algorithms tailored for the special characteristics of FD.

ACKNOWLEDGEMENTS

This work was supported in part by the NSF grant ECCS-1547406, the Qualcomm Innovation Fellowship, and the People Programme (Marie Curie Actions) of the European Union's Seventh Framework Programme (FP7/2007-2013) under REA grant agreement n^{o}[PIIF-GA-2013-629740].11. We thank Jin Zhou and Harish Krishnaswamy for providing us with the cancellation data from [7].

REFERENCES

[1] J. Marašević and G. Zussman, "On the capacity regions of single-channel and multi-channel full-duplex links," in *Proc. ACM MobiHoc'16*, 2016.

[2] A. Sabharwal, P. Schniter, D. Guo, D. Bliss, S. Rangarajan, and R. Wichman, "In-band full-duplex wireless: Challenges and opportunities," *IEEE J. Sel. Areas Commun.*, vol. 32, no. 9, pp. 1637–1652, Sept. 2014.

[3] J. Choi, M. Jain, K. Srinivasan, P. Levis, and S. Katti, "Achieving single channel, full duplex wireless communication," in *Proc. ACM MobiCom'10*, 2010.

[4] M. Jain, J. Choi, T. Kim, D. Bharadia, S. Seth, K. Srinivasan, P. Levis, S. Katti, and P. Sinha, "Practical, real-time, full duplex wireless," in *Proc. ACM MobiCom'11*, 2011.

[5] M. Khojastepour, K. Sundaresan, S. Rangarajan, X. Zhang, and S. Barghi, "The case for antenna cancellation for scalable full-duplex wireless communications," in *Proc. ACM HotNets'11*, 2011.

[6] E. Aryafar, M. A. Khojastepour, K. Sundaresan, S. Rangarajan, and M. Chiang, "MIDU: enabling MIMO full duplex," in *Proc. ACM MobiCom'12*, 2012.

[7] J. Zhou, T. H. Chuang, T. Dinc, and H. Krishnaswamy, "Integrated wideband self-interference cancellation in the RF domain for FDD and full-duplex wireless," *IEEE J. Solid-State Circuits*, vol. 50, no. 12, pp. 3015–3031, Dec. 2015.

[8] D. Bharadia, E. McMilin, and S. Katti, "Full duplex radios," in *Proc. ACM SIGCOMM'13*, 2013.

[9] M. Duarte, C. Dick, and A. Sabharwal, "Experiment-driven characterization of full-duplex wireless systems," *IEEE Trans. Wireless Commun.*, vol. 11, no. 12, pp. 4296–4307, 2012.

[10] E. Ahmed, A. M. Eltawil, and A. Sabharwal, "Rate gain region and design tradeoffs for full-duplex wireless communications," *IEEE Trans. Wireless Commun.*, vol. 12, no. 7, pp. 3556–3565, 2013.

[11] W. Li, J. Lilleberg, and K. Rikkinen, "On rate region analysis of half-and full-duplex OFDM communication links," *IEEE J. Sel. Areas Commun.*, vol. 32, no. 9, pp. 1688–1698, Sept. 2014.

[12] W. Cheng, X. Zhang, and H. Zhang, "Optimal dynamic power control for full-duplex bidirectional-channel based wireless networks," in *Proc. IEEE INFOCOM'13*, 2013.

[13] J. Marašević, J. Zhou, H. Krishnaswamy, Y. Zhong, and G. Zussman, "Resource allocation and rate gains in practical full-duplex systems," *IEEE/ACM Trans. Netw.*, vol. 25, no. 1, pp. 292–305, 2017.

[14] W. Bi, X. Su, L. Xiao, and S. Zhou, "On rate region analysis of full-duplex cellular system with inter-user interference cancellation," in *Proc. IEEE ICCW'15*, 2015.

[15] D. Korpi, T. Riihonen, and M. Valkama, "Achievable rate regions and self-interference channel estimation in hybrid full-duplex/half-duplex radio links," in *Proc. IEEE CISS*, 2015.

[16] G. Zheng, "Joint beamforming optimization and power control for full-duplex MIMO two-way relay channel," *IEEE Trans. Signal Process.*, vol. 63, no. 3, pp. 555–566, 2015.

[17] J. Marašević and G. Zussman, "On the capacity regions of single-channel and multi-channel full-duplex links," May 2016, arXiv preprint, http://arxiv.org/abs/1605.07559.

[18] J. Bai and A. Sabharwal, "Distributed full-duplex via wireless side-channels: Bounds and protocols," *IEEE Trans. Wireless Commun.*, vol. 12, no. 8, pp. 4162–4173, 2013.

[19] X. Xie and X. Zhang, "Does full-duplex double the capacity of wireless networks?" in *Proc. IEEE INFOCOM'14*, 2014.

[20] Y. Yang and N. B. Shroff, "Scheduling in wireless networks with full-duplex cut-through transmission," in *Proc. IEEE INFOCOM'15*, 2015.

[21] T. H. Cormen, C. E. Leiserson, R. L. Rivest, and C. Stein, *Introduction to Algorithms, Third Edition*, 3rd ed. The MIT Press, 2009.

[22] J. M. Ortega and W. C. Rheinboldt, *Iterative solution of nonlinear equations in several variables*. Academic Press, 1970.

[23] A. Beck, "On the convergence of alternating minimization for convex programming with applications to iteratively reweighted least squares and decomposition schemes," *SIAM J. Optimiz.*, vol. 25, no. 1, pp. 185–209, 2015.

[24] J. Gorski, F. Pfeuffer, and K. Klamroth, "Biconvex sets and optimization with biconvex functions: a survey and extensions," *Math. Method. Oper. Res.*, vol. 66, no. 3, pp. 373–407, 2007.

[25] J. Huang, V. G. Subramanian, R. Agrawal, and R. A. Berry, "Downlink scheduling and resource allocation for OFDM systems," *IEEE Trans. Wireless Commun.*, vol. 8, no. 1, pp. 288–296, Jan. 2009.

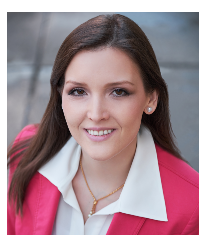

Jelena Diakonikolas received the Ph.D. degree in Electrical Engineering from Columbia University in 2016. She is currently a Postdoctoral Associate at Boston University. Her research focuses on continuous and discrete optimization, with applications in wireless networks. Jelena is a recipient of the Morton B. Friedman Prize for Excellence at Columbia Engineering. She is a co-winner of the Qualcomm Innovation Fellowship 2015 award and was listed as one of the "10 Women in Communications/Networking That You Should Watch" by N^2 Women in 2016.

Gil Zussman received the Ph.D. degree in Electrical Engineering from the Technion in 2004 and was a postdoctoral associate at MIT in 2004-2007. He is currently an Associate Professor of Electrical Engineering at Columbia University. His research interests are in the areas of wireless, mobile, and resilient networks. Gil is a co-recipient of 7 best paper awards, the Fulbright Fellowship, the DTRA Young Investigator Award, and the NSF CAREER Award.

APPENDIX

A. Omitted Proofs from Section IV

Proof of Corollary 4.3: From the proof of Lemma 4.2, for $r_m(r_b)$ to be concave in all $r_b \in [0, s_b]$, the quadratic function (10) in α_b needs to be non-positive for all $\alpha_b \in [0, 1]$. It follows that the discriminant of (10) must be positive and the larger of the roots, α_b^+, must be greater than or equal to 1 (the smaller root is negative). Finding the larger root of (10) gives:

$$\alpha_b^+ = \frac{1+\overline{\gamma_{mm}}}{\overline{\gamma_{bm}}}\Bigg(-1 + \sqrt{1+\frac{(\overline{\gamma_{bm}})^2}{(\overline{\gamma_{bb}})^2}\cdot\frac{1+\overline{\gamma_{mb}}}{(1+\overline{\gamma_{mm}})^2} - \frac{\overline{\gamma_{bm}}}{\overline{\gamma_{bb}}}\cdot\frac{2+\overline{\gamma_{mb}}}{1+\overline{\gamma_{mm}}}}\Bigg) \geq 1. \tag{26}$$

From (26), as $\alpha_b^+ > 0$, it must also be:

$$\frac{(\overline{\gamma_{bm}})^2}{(\overline{\gamma_{bb}})^2}\cdot\frac{1+\overline{\gamma_{mb}}}{(1+\overline{\gamma_{mm}})^2} - \frac{\overline{\gamma_{bm}}}{\overline{\gamma_{bb}}}\cdot\frac{2+\overline{\gamma_{mb}}}{1+\overline{\gamma_{mm}}} > 0$$
$$\Rightarrow \quad \overline{\gamma_{bm}} > \overline{\gamma_{bb}}(1+\overline{\gamma_{mm}})\cdot\frac{2+\overline{\gamma_{mb}}}{1+\overline{\gamma_{mb}}}. \tag{27}$$

Note that (27) implies that the discriminant of (10) is greater than 1 and therefore positive.

Further, solving (26) for $\overline{\gamma_{bm}}$, we get:

$$\frac{1+\overline{\gamma_{mm}}}{\overline{\gamma_{bm}}}\Bigg(-1 + \sqrt{1+\frac{(\overline{\gamma_{bm}})^2}{(\overline{\gamma_{bb}})^2}\cdot\frac{1+\overline{\gamma_{mb}}}{(1+\overline{\gamma_{mm}})^2} - \frac{\overline{\gamma_{bm}}}{\overline{\gamma_{bb}}}\cdot\frac{2+\overline{\gamma_{mb}}}{1+\overline{\gamma_{mm}}}}\Bigg) \geq 1$$
$$\Leftrightarrow \frac{\overline{\gamma_{bm}}}{1+\overline{\gamma_{mm}}}\left(\frac{1+\overline{\gamma_{mb}}}{(\overline{\gamma_{bb}})^2}-1\right) - \frac{2+\overline{\gamma_{mb}}}{\overline{\gamma_{bb}}} - 2 \geq 0. \tag{28}$$

Now, for (28) to be possible to satisfy, as $\overline{\gamma_{bb}}, \overline{\gamma_{mm}}, \overline{\gamma_{bm}}, \overline{\gamma_{mb}}$ are all strictly positive, it must be:

$$\frac{1+\overline{\gamma_{mb}}}{(\overline{\gamma_{bb}})^2} - 1 > 0 \quad \Rightarrow \quad \overline{\gamma_{mb}} > (\overline{\gamma_{bb}})^2 - 1. \tag{29}$$

Finally, solving (28) (given that (29) holds), we get:

$$\overline{\gamma_{bm}} \geq (1+\overline{\gamma_{mm}})\frac{2+\frac{2+\overline{\gamma_{mb}}}{\overline{\gamma_{bb}}}}{\frac{1+\overline{\gamma_{mb}}}{(\overline{\gamma_{bb}})^2}-1}. \tag{30}$$

Inequalities (27), (29), and (30) and their counterparts obtained when $r_b(r_m)$ is concave give (11)–(12) from the statement of the corollary. ∎

B. Single-Channel TDFD Algorithm Pseudocode

Algorithm 9 SC-TDFDREGION(r_b^*)

Input: $\overline{\gamma_{mb}}, \overline{\gamma_{bm}}, \overline{\gamma_{mm}}, \overline{\gamma_{bb}}$
$s_b = \log(1+\frac{\overline{\gamma_{bm}}}{1+\overline{\gamma_{mm}}})$, $s_m = \log(1+\frac{\overline{\gamma_{mb}}}{1+\overline{\gamma_{bb}}})$
$\overline{r_b} = \log(1+\overline{\gamma_{bm}})$, $\overline{r_m} = \log(1+\overline{\gamma_{mb}})$
Run SC-RR-SHAPE to determine $\mathcal{S}_b, r_b^+, \mathcal{S}_m, r_m^+$
if $\mathcal{S}_b = [1,1]$ and $\mathcal{S}_b = [1,1]$ **then**
  r_m^* =SC-FD-REGION(r_b^*)
else
  if $\mathcal{S}_b = [0,0]$ and $\mathcal{S}_b = [0,0]$ **then**
    if $s_b + s_m \geq \max\{\overline{r_b}, \overline{r_m}\}$ **then**
      if $r_b \leq s_b$ **then**
        $\alpha = r_b^*/s_b$, $r_m^* = (1-\alpha)\overline{r_m} + \alpha s_m$
      else
        $\alpha = (\overline{r_b} - r_b^*)/(\overline{r_b} - s_b)$, $r_m^* = (1-\alpha)s_m$
    else
      $\alpha = r_b^*/\overline{r_b}$, $r_m^* = (1-\alpha)\overline{r_m}$
  else
    if $s_b + s_m \geq \max\{\overline{r_b}, \overline{r_m}\}$ **then**
      if $r_b \leq s_b$ **then**
        Via a binary search for $r_b' \in [0, r_b^+]$, find r_b' such that the line through (s_b, s_m) and $(r_b', r_m(r_b'))$ is tangent to $\mathcal{S}_b$
        if $r_b^* \leq r_b'$ **then**
          r_m^* =SC-FD-REGION(r_b^*)
        else
          $\alpha = (r_b^* - r_b')/(s_b - r_b')$
          $r_m^* = (1-\alpha)r_m(r_b') + \alpha s_m$
      else
        Via a binary search for $r_m' \in [0, r_m^+]$, find r_m' such that the line through (s_b, s_m) and $(r_b(r_m'), r_m')$ is tangent to $\mathcal{S}_m$
        if $r_b^* \geq r_b(r_m')$ **then**
          r_m^* =SC-FD-REGION(r_b^*)
        else
          $\alpha = (r_b^* - s_b)/(r_b(r_m') - s_b)$
          $r_m^* = (1-\alpha)r_m' + \alpha s_m$
    else
      if $S_b = [1,0]$ **then**
        Via a binary search for $r_b' \in [0, r_b^+]$, find r_b' such that the line through $(\overline{r_b}, 0)$ and $(r_b', r_m(r_b'))$ is tangent to $\mathcal{S}_b$
        if $r_b^* \leq r_b'$ **then**
          r_m^* =SC-FD-REGION(r_b^*)
        else
          $\alpha = (r_b^* - r_b')/(\overline{r_b} - r_b')$
          $r_m^* = (1-\alpha)r_m(r_b')$
      else
        Via a binary search for $r_m' \in [0, r_m^+]$, find r_m' such that the line through (s_b, s_m) and $(r_b(r_m'), r_m')$ is tangent to $\mathcal{S}_m$
        if $r_b^* \geq r_b(r_m')$ **then**
          r_m^* =SC-FD-REGION(r_b^*)
        else
          $\alpha = (r_b^* - \overline{r_b})/(r_b(r_m') - \overline{r_b})$
          $r_m^* = (1-\alpha)r_m'$
return r_m^*